Galaxy Discs as Accretion Discs

Master's thesis in Physics & Astronomy

Bergur Halldórsson
Supervisor: Alessandro Romeo

Department of Space, Earth and Environment
CHALMERS UNIVERSITY OF TECHNOLOGY
Gothenburg, Sweden 2021

Master's thesis 2021:NN

Galaxy Discs as Accretion Discs

Bergur Halldórsson
Supervisor: Alessandro Romeo

CHALMERS
UNIVERSITY OF TECHNOLOGY

Department of Space, Earth and Environment
Chalmers University of Technology
Gothenburg, Sweden 2021

Galaxy Discs as Accretion Discs
Bergur Halldórsson

Supervisor: Alessandro Romeo

Master's Thesis 2021:NN
Department of Space, Earth and Environment
Chalmers University of Technology
SE-412 96 Gothenburg
Telephone +46 31 772 1000

Cover: Hubble image of NGC 2841, one of the galaxies examined in the thesis. Blue stars indicate the tightly wound spiral arms Source: https://hubblesite.org/image/3845/

Typeset in LaTeX
Gothenburg, Sweden 2021

Galaxy Discs as Accretion Discs
Bergur Halldórsson
Department of Earth, Space and Environment
Chalmers University of Technology

Abstract

Accretion and accretion discs around compact objects such as black holes and neutron stars are well studied phenomena, but galactic discs have rarely been examined as accretion discs, despite showing clear evidence of radial mass inflow. Rotation curves, radial velocity and radial mass flux data for ten different spiral galaxies were acquired from Schmidt et al. (2016) who in turn were working with data from The HI Nearby Galaxy Survey (THINGS). The data are used to calculate several quantities which are essential for accurately modelling accretion discs, with a focus on two different versions of the α parameter, which describes the efficiency with which turbulence acts as a source of "effective" viscosity in the accretion process. These quantities are then analysed with consideration for the properties of the galaxies and the structures present. While there was no obvious connection found between the value of α and the spiral structure present throughout the disc structures with clearer radial limits such as rings and bars were found to have definite effects on the value of α.

Keywords: alpha-disc model, Spiral galaxies

Acknowledgements

I would like to sincerely thank my supervisor, Alessandro Romeo, for his guidance and feedback as well as his incredible patience and generosity as the work on the thesis dragged on. Without him, this thesis would have been neither attempted nor completed.
Secondly, I would like to thank the Department of Space, Earth and Environment at Chalmers for their support and understanding in covid-times. I would also like to thank Helgi Þórsson and Sóley Halldórsdóttir for proofreading at the last stages. Last but not least, I would like to thank Tobias M. Schmidt, Frank Bigiel, Ralf S. Klessen and W. J. G de Blok for the use of their data, which this thesis builds on.

Bergur Halldórsson, Reykjavík, January 21

Contents

List of Figures

List of Tables

1
Introduction

Accretion is a fundamental process that occurs in all sorts of astrophysical systems and often results in a disc of material surrounding a massive body. While these discs vary in many ways, such as scale, type of central body and force powering accretion, the basic mechanics remain similar.
There have been quite extensive studies into the accretion discs surrounding supermassive black holes at the center of galaxies. Similarly, protoplanetary discs and other stellar scale accretion discs have been the subject of much research. Galactic discs, however, have rarely been studied specifically as a form of accretion disc, despite the fact that they show much of the same behavior.
There is now reliable observational evidence of radial mass inflow in galaxy discs (see Fig. 1.1). The idea behind this master's thesis project is to use these observations, together with the simple but predictive Shakura-Sunyaev accretion disc model, well known in the context of accretion discs around compact objects, to constrain the physics of mass, angular momentum and energy transport in spiral galaxies.
The structure of the thesis is as follows. Chapter 2 establishes the theoretical framework behind the work. It explains the meaning of the quantities studied and the methods with which they were calculated. Chapter 3 discusses the work of Schmidt et al. (2016), the source of the data used here, as well as showing said data. Chapter 4 describes the calculations in some detail using NGC 3198 as an example before showing the calculated output quantities and discussing the quality of the results. Chapter 5 then contains a discussion of the results and their implications. Finally chapter 6 concludes the thesis and discusses the possibilities for future research on this topic.

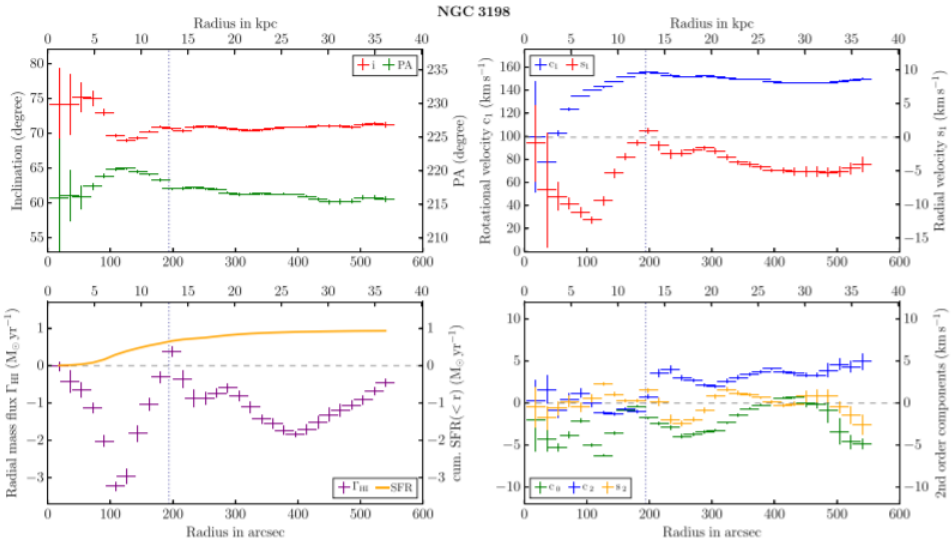

Figure 1.1: Observed radial mass inflow in the spiral galaxy NGC 3198 (Schmidt et al., 2016) This is one of the 10 spiral galaxies for which Schmidt et al. (2016) derived radial velocities and mass fluxes. In this thesis I will use all such data to achieve a better understanding of galaxy discs as accretion discs.

2

Theoretical Framework

The theory behind the study is explained here, giving a brief explanation of accretion before going into the reason for disc formation. The various quantities of note are explained, ending with the α parameter, commonly used in accretion disc theory and the subject of most of the analysis in the later chapters of the thesis. Many of the equations shown here come or are derived from Shu (1991), but some very important equations are taken from Pringle (1981) and Romeo (1992).

Accretion and the thin-disc approximation Accretion is, in the simplest of terms, the inflow of material towards a massive central body due to gravity. Most objects of interest in astrophysics are formed by accretion, but accretion discs are structures sustained by these processes. In this case, our focus is on galactic discs, which are functionally accretion discs, although their vast scale as well as the size and low density of their constituent "particles", i.e. stars makes them somewhat different from more conventional accretion disc systems. We assume that the vertical scale of the disc is far smaller than the radial extent, in other words $H << R$, where H is the scale height and R is the radius. This is the thin-disc approximation, and it is useful in the study of many, but not all accretion discs. All of the galaxies studied here are spirals, and in their case the validity of this approximation is easy to see.

Why do discs form? A system consists of a cloud of gas particles rotating in a potential well. The particles will collide and lose energy while the overall angular momentum remains unchanged. The orbit of least energy for a given angular momentum is circular so the particles end up in circular orbits, and since a system with fewer collisions is more stable, over time the orbits tend to end up in the same plane in nonintersecting orbits. The result is a flat disc. This is covered in more detail in Pringle (1981).

Angular velocity and momentum. Smaller accretion discs formed around a more massive central object are generally Keplerian, with shear forces between material elements at different radii travelling with different angular velocities,

$$\Omega(R) = \frac{v_\phi(R)}{R}. \tag{2.1}$$

In eq. 2.1, $v_\phi(R)$ is the rotation velocity and is unsurprisingly the radius. With the shape of the disc, cylindrical coordinates are the natural choice.

Interaction between adjacent radial elements causes a transport of the angular momentum,

$$J(R) = R^2\Omega = Rv_\phi(R), \tag{2.2}$$

from the inner element to the outer one.

The mass flow rate. In these calculations it is important to note the radial mass flow rate, the amount of material flowing either in or out of a circle with a given radius per unit time.

$$\dot{M}(R) = -2\pi R v_R(R)\Sigma(R), \tag{2.3}$$

where $\Sigma(R)$ is the surface density of the disc. The data used in our calculations include $\dot{M}(R)$ but not Σ, so this equation is used to calculate the surface density from the mass flow rate, rather than the other way around:

$$\Sigma(R) = -\frac{\dot{M}(R)}{2\pi R v_R(R)}. \tag{2.4}$$

This is used to compare the data we use to another set of data to ensure its reliability.

Torque. Torque is of course closely connected with the angular momentum and is an essential part of our calculations. It is calculated here using the angular momentum transport equation to find the derivative,

$$-\dot{M}(R)\frac{dJ(R)}{dR} = \frac{d\mathcal{T}(R)}{dR}, \tag{2.5}$$

which is then integrated.

$$\mathcal{T}(R) = \int_0^R \frac{d\mathcal{T}(R)}{dR}dR = -\int_0^R \dot{M}(R)\frac{dJ(R)}{dR}dR \tag{2.6}$$

The kinematic viscosity. Friction offers a simple explanation of the shear, but it can be shown that the friction between the molecules, the molecular viscosity, is a very small part of the overall effective viscosity in accretion discs. Using rather typical values for a stellar accretion disc as calculated in Ryden (2011), it can be demonstrated that the accretion time with molecular viscosity alone would be greater than the age of the universe, but we know from observations that the true accretion timescale is significantly shorter.
Note that we use the kinematic viscosity ν, defined as the ratio between the dynamic viscosity and density of the material, $\nu \equiv \mu/\rho$. Instabilities and turbulence often appear in these discs, and can create a much larger effective kinematic viscosity. In smaller discs, these may be magnetic, hydrodynamical or gravitational in origin. Galactic discs are in this sense relatively simple, as stars within them only interact gravitationally. That said, there are many different ways for gravity to affect the effective kinematic viscosity, including gravitational instabilities and turbulence, as well as the non-axisymmetric structures such as spiral arms and central bars. Because of this, accurately predicting their impact is extremely difficult. With the quantities we already have, we can calculate the effective kinematic viscosity based

on observational data without having to worry too much about the exact processes behind it using equation 2.7,

$$\nu(R) = \frac{\mathcal{T}(R)}{2\pi R^3 \frac{d\Omega(R)}{dR}\Sigma(R)}, \tag{2.7}$$

which is from Shu (1991) and is derived from eq. 2.6
There are gravitational instabilities and turbulence, as well as the non-axisymmetric structures commonly seen in spiral galaxies .

An elaboration on the scale height. Early in this chapter, the scale height H was mentioned in the context of the thin-disc approximation, but was not explained in depth. Scale height in the context of accretion discs is the distance from the midplane over which the pressure or density drops by a factor of e. It is used to evaluate the vertical thickness of the disc since there is no clear boundary. Romeo (1992) shows that the scale height can be calculated from quantities we already have using the following equation.

$$H(R) = \frac{\sigma^2(R)}{(2)\pi G\Sigma_{tot}(R)}. \tag{2.8}$$

σ is the velocity dispersion of the disc, which is easily found from the radial velocity.

The α-disc model. This model originates in Shakura & Sunyaev (1973) and is very useful for describing accretion discs. The viscosity from turbulence in the disc is described using the following:

$$\nu = \alpha c_s H. \tag{2.9}$$

c_s is the sound speed in the material, and α is a parameter with a value of up to 1. This allows us to essentially replace the complicated turbulent viscosity with the simple parameter α and therefor accurately model accretion discs without having to delve into the precise details of turbulence, which are generally impractically complicated.
There are two different values of α calculated here. The former, α_1, is commonly used in the study of accretion while the latter applies specifically to multicomponent self-gravitating discs such as galactic discs and is very relevant to this thesis.
Starting with α_1, assume there is powerful fluid turbulence and correlation between its R and ϕ components, the shear stress for the fluctuating velocity field can be described with $\pi_{R\phi} = -\rho\alpha_1\sigma^2$. The shear stress can also be expressed as being proportional to the strain rate with the dynamical viscosity as as the proportionality factor, $\pi_{R\phi} = \mu R\frac{d\Omega}{dR}$. Replacing μ with ν via the definition $\nu \equiv \mu/\rho$ given earlier and combining these two equations results in an expression of α_1 relying only on previously defined quantities:

$$\alpha_1(R) = -\frac{R\frac{d\Omega(R)}{dR}\nu(R)}{\sigma^2(R)} \tag{2.10}$$

The expression for α_2 is easier to derive. It is calculated from eq. 2.9, using the velocity dispersion of the galaxy instead of the sound speed.

$$\alpha_2(R) = \frac{\nu(R)}{\sigma(R)H(R)}. \tag{2.11}$$

The two α parameters can be used to get an idea of the effective viscosity and the accretion efficiency at various radii throughout the disc and allows for comparison between galaxies. We'll be able to study the effect of structures on α and analyze how α in galaxies compares to α in smaller, more typical accretion discs.

3

Galaxy Sample, Data and Method

´

Much of the data used in the thesis comes from Schmidt et al. (2016). Here some relevant points in that paper are summarized and then the input data is plotted. Schmidt et al. used data from The HI Nearby Galaxy Survey (THINGS), collected using the Very Large Array, to look for radial flows in the galactic discs of ten galaxies using 21 cm line observations of atomic hydrogen. Using this data and new methods to analyze it, they were able to find previously undetected radial flows.
The survey contains 34 galaxies, but not all of them were suitable. The ones that were studied had to be well resolved, had to have inclinations greater than $30 - 40$ and had to have relatively regular velocity fields. In the end, Schmidt et. al. ended up with 10 suitable galaxies, which are the ones used in this thesis. All of them have distances between 3 and 15 Mpc, giving a resolution of $100 - 500pc$.
They then studied different methods for modelling the velocity fields of galaxies based on the line-of-sight velocity observed. There are two methods available, which they combined to get an accurate model. The first is a tilted ring model, where the disc is treated as a series of concentric rings, with the measured line-of-sight velocity defined as

$$V_{los} = V_{sys} + V_{rot}sin(i)cos(\theta) + V_{rad}sin(i)sin(\theta), \tag{3.1}$$

where V_{sys} is the systematic velocity of the galaxy with respect to the observer, i is the inclination angle of the galaxy, and θ is the azimuthal angle. This allows for measurement of both rotational and radial velocities as a function of radius, but is limited by the fact that it assumes radial symmetry around the galactic center. This can be mitigated by the second method, which is a Fourier decomposition. It is possible to allow V_{rot} and V_{rad} to depend on θ, however there aren't enough observables available to determine those quantities as arbitrary functions, so $V_{rot}(\theta)$ and $V_{rad}(\theta)$ are described as Fourier series. This method was described in detail in the paper.
There are two problems with these methods. The first is that within each ring, the parameters are all considered independent of radius, which prevents the data from fitting perfectly in the inner part of the galaxy. The second is that solid-body rotation makes it impossible to disentangle V_{rot} and $sin(i)$. This causes problems where rotation curves rise linearly, namely dwarf galaxies and the inner part of spirals. As the paper mainly studied the outer disk, neither of these issues were particularly relevant there, but some of the most interesting results of this thesis are in the inner part of the disc so the methods used may not be ideal for the research being done here.

They found that the radial motions of material in the disc must be considered during the tilted ring fitting, it's not enough to add that later with the Fourier decomposition. They also found that it is very difficult to include terms above second-order in the Fourier decomposition due to degeneracy between the c_3 component of the decomposition and the inclination angle. As a result they only included terms up to second order. The model they ended up using has the following form:

$$V_{los} = V_{sys} + sin(i)[c_0 + s_1 sin(\theta) + c_1 cos(\theta) + s_2 sin(2\theta) + c_2 cos(2\theta)]. \tag{3.2}$$

The rings they used overlap because in the case of warped discs gaps can appear. As a result, there is some correlation between adjacent rings, but it is mentioned that it is possible to get a statistically independent sample by using only every other ring. The net mass flow rate was obtained using

$$\Gamma_{rad}(R) = \int_0^{2\pi} V_{rad}(R,\phi)\Sigma_{HI}(R,\phi)Rd\phi. \tag{3.3}$$

In its simplest form, the mass flow rate is obtained by simply multiplying together the radial velocity of the material and its surface density. The mass flow plotted below is different from Γ_{rad} by a factor of -1.36 since Γ_{rad} only includes HI and treats outflow as positive. The sign is changed to have the inflow positive, since we are more interested in that, and the factor 1.36 allows us to approximate all of the material in the galactic disc.
The relevant results are plotted below. There are four basic quantities of interest, the orbital velocity $v_\phi(R)$, radial velocity $v_r(R)$, mass flow rate $\dot{M}(R)$ and star formation rate, all of which are given as functions of radius. Two other sets of data were used as well, surface density values from Leroy et al. (2008) and velocity dispersion data from Romeo & Mogotsi (2017). Those quantities are not plotted here, but are brought up in more detail in the next chapter. All four plots for each galaxy include the data from Schmidt et al. in red, but the velocity curve also includes a fit from Leroy et al. as a dashed blue line, and a fit made using the same equation, but with new parameters calculated to better fit the observational data we have. The equation used is

$$v_\phi(R) = v_{flat}\left[1 - exp\left(\frac{-R}{l_{flat}}\right)\right] \tag{3.4}$$

where the parameters are v_{flat} and l_{flat}, the former describing the velocity at which the curve is flat, and the latter the length scale to reach that state.

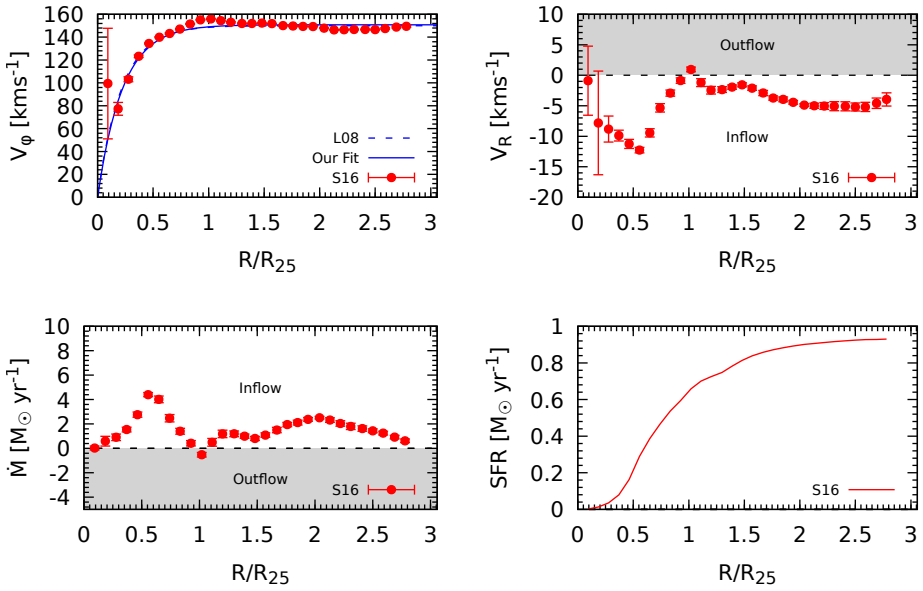

Figure 3.1: The input data for NGC 3198. The radius of the ring is shown in orange, and the maximum radius of the bar is shown in purple.

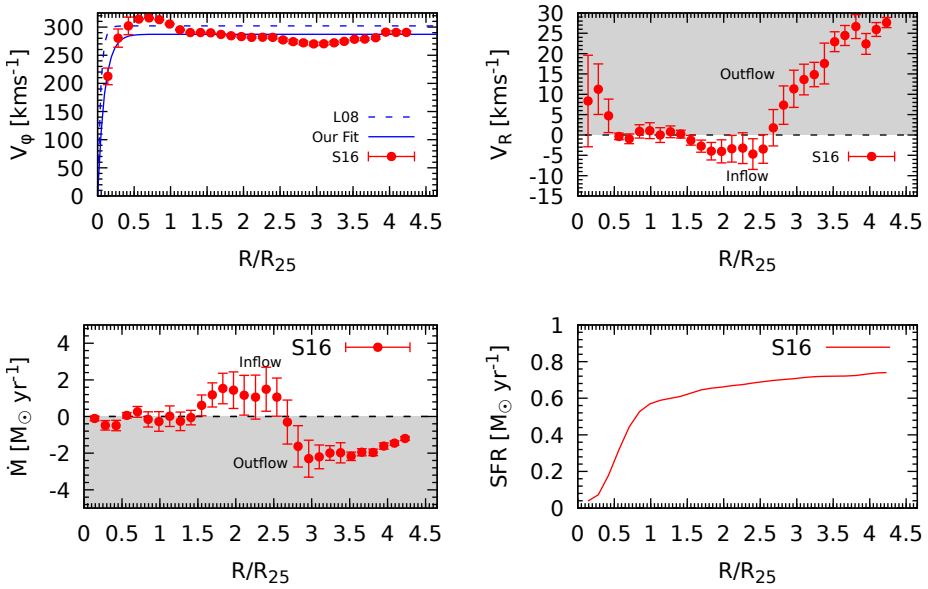

Figure 3.2: The input data for NGC 2841.

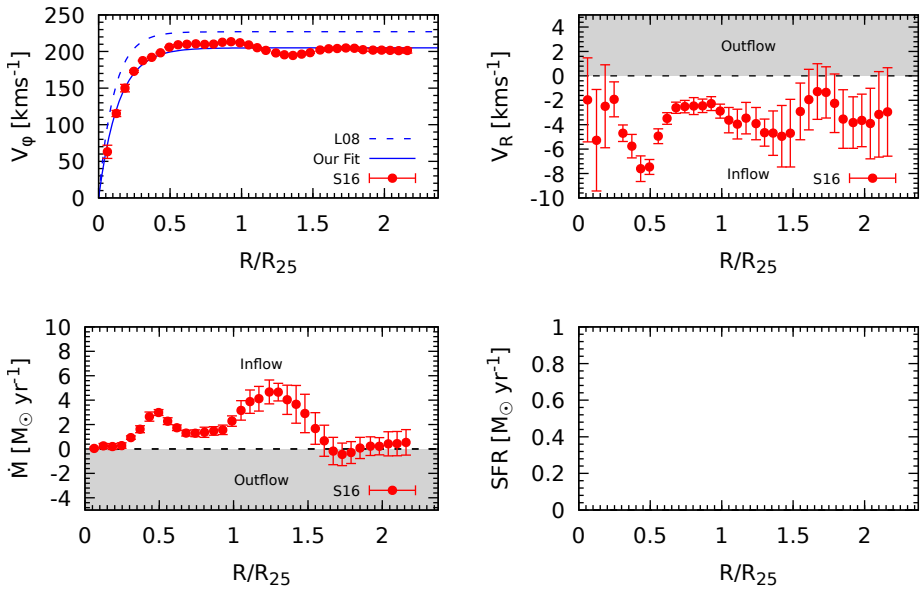

Figure 3.3: The input data for NGC 3521. The SFR data is missing for this galaxy.

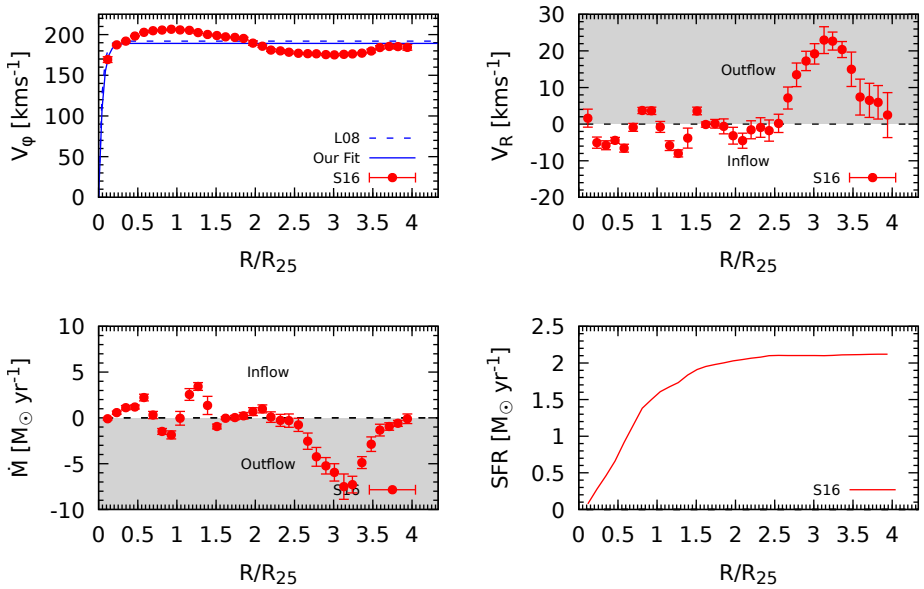

Figure 3.4: The input data for NGC 5055.

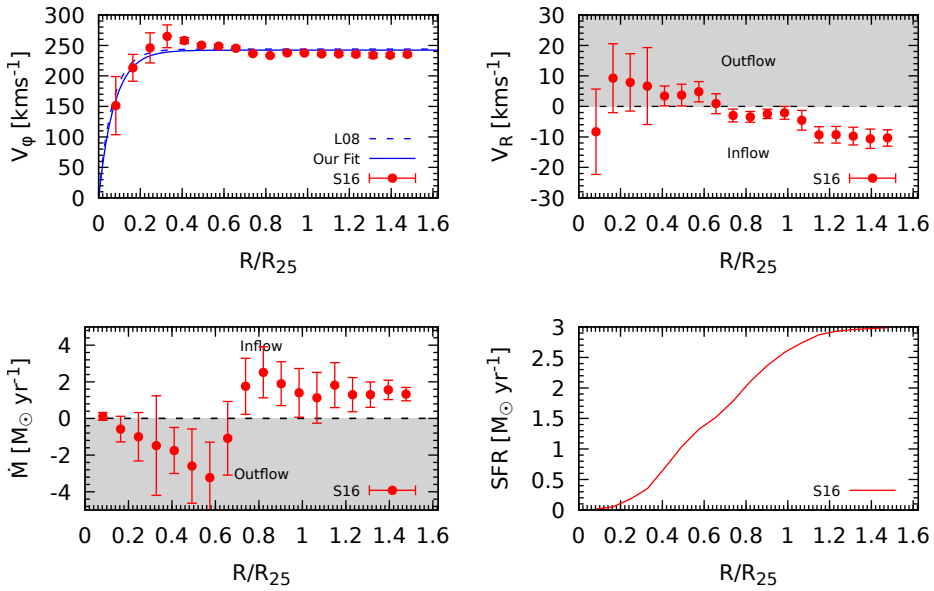

Figure 3.5: The input data for NGC 7331.

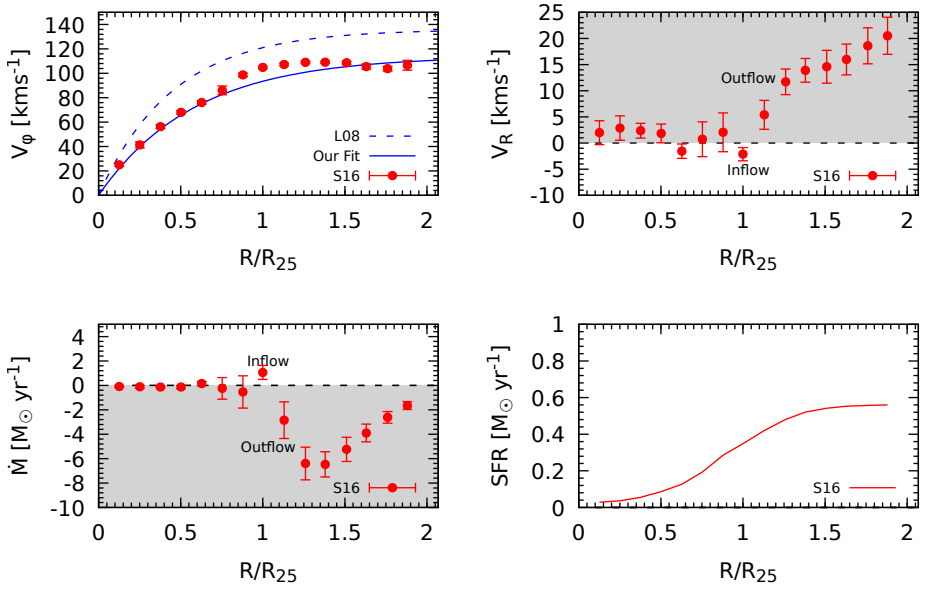

Figure 3.6: The input data for NGC 925.

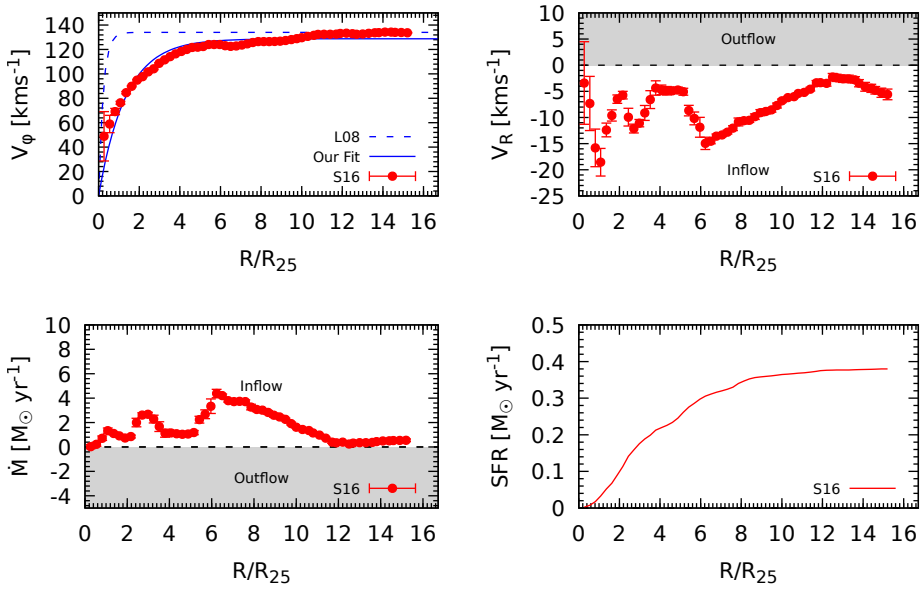

Figure 3.7: The input data for NGC 2403.

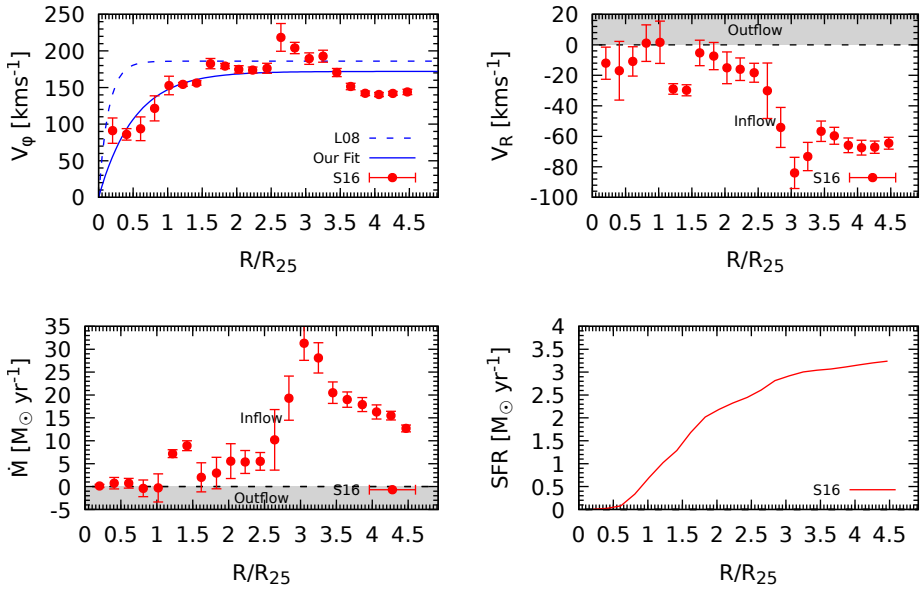

Figure 3.8: The input data for NGC 6946.

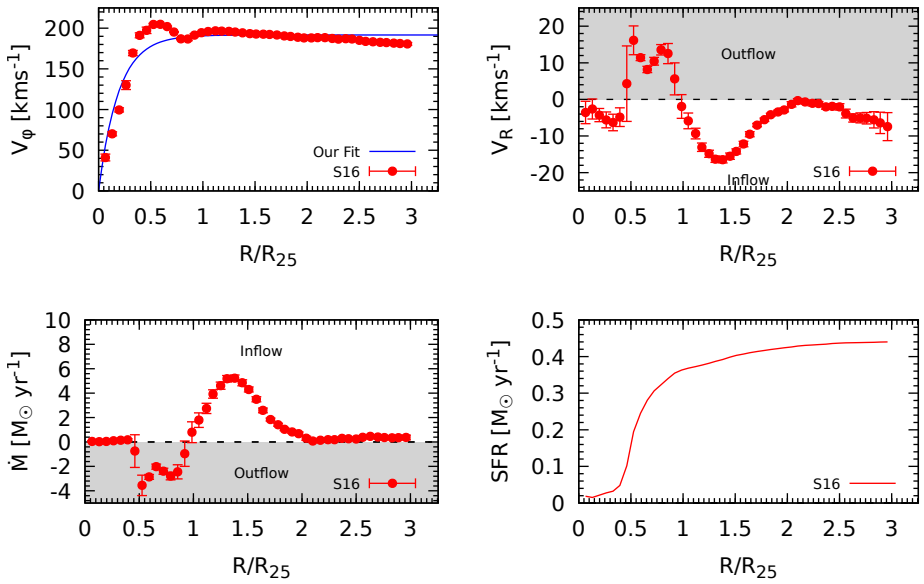

Figure 3.9: The input data for NGC 2903.

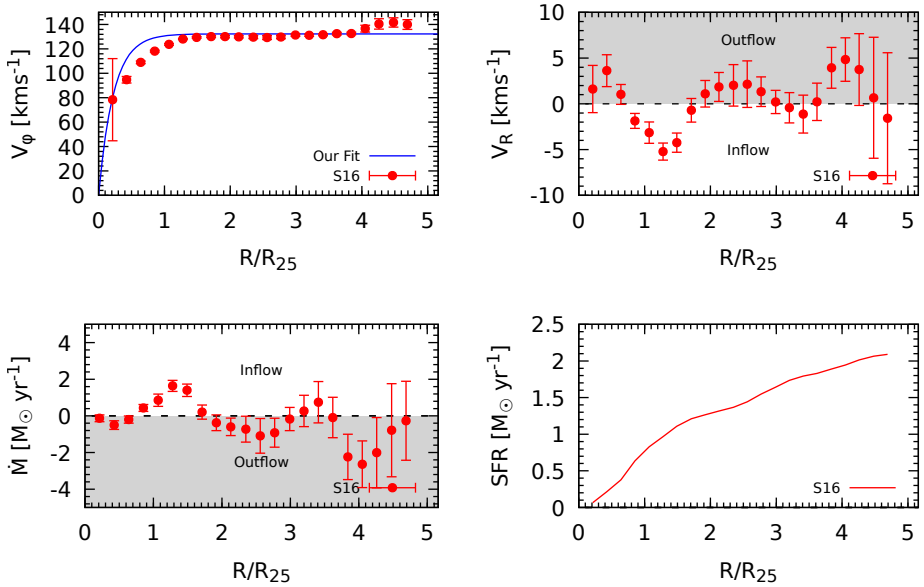

Figure 3.10: The input data for NGC 3621.

4

Results

4.1 Summary of input and output quantities

In chapter 2, we first established the input quantities acquired from Schmidt et al. Schmidt et al. (2016):

- Angular velocity $v_\phi(R)$
- Radial velocity $v_r(R)$
- Mass flow rate $\dot{M}(R)$
- Star formation rate $SFR(R)$

We then established the following output quantities:

- Angular momentum $J(R) = Rv_\phi(R)$
- Angular velocity $\Omega(R) = v_\phi(R)/R$
- Surface density $\Sigma(R) = -\frac{\dot{M}(R)}{2\pi R v_R(R)}$
- Torque derivative $\frac{d\mathcal{T}(R)}{dR} = -\dot{M}(R)\frac{dJ(R)}{dR}$
- Torque $\mathcal{T}(R) = \int \frac{d\mathcal{T}(R)}{dR}dR = -\int \dot{M}(R)\frac{dJ(R)}{dR}dR$
- Kinematic viscosity $\nu(R) = \frac{\mathcal{T}(R)}{2\pi R^3 \frac{d\Omega(R)}{dR}\Sigma(R)}$
- $\alpha_1(R) = -\frac{R\frac{d\Omega(R)}{dR}\nu(R)}{\sigma^2(R)}$
- Scale height $H(R) = \frac{\sigma^2(R)}{(2)\pi G\Sigma_{tot}(R)}$
- $\alpha_2(R) = \frac{\nu(R)}{\sigma(R)H(R)}$

In this chapter, we will look at ten galaxies, and these quantities are all plotted for each one. The first is NGC 3198, which is used as a case study to discuss the process in more detail. The rest of the galaxies and their data are described and the plots are shown at the end.

4.2 A case study: NGC 3198

NGC 3198 appears to be one of the best galaxies sampled here with regards to data quality. We have all of the data we want, unlike some of the other galaxies. The different data sources also seem to largely agree, which is a sign of reliability. As such, it is a great example to use for explaining the calculations done for all ten of the galaxies and the results of the calculations.

For a bit of background, NGC 3198 is a barred spiral galaxy approximately 14.7 Mpc away, with loosely wound spiral arms and a weak ring structure that has a radius of about $3.563kpc$. (Corradi et al., 1991) It has an optical radius of $12.96kpc$. The bar is inside the ring and is rather weak. (Daod & Zeki, 2019).

Fig. 4.1 shows the first few output values for NGC 3198. The angular momentum per unit mass $J = Rv_\phi$, the angular velocity $\Omega = v_\phi/R$, and their derivatives are all shown. The orange line shows the radius of the ring, while the radial extent of the bar is shown in purple. This color coding is used consistently in the following plots. The blue lines show the same quantities calculated from the rotation curve

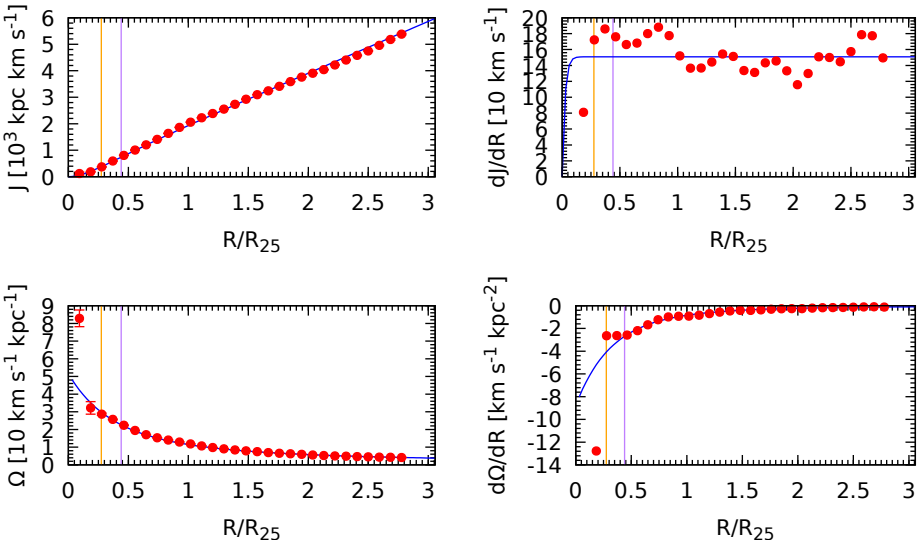

Figure 4.1: The angular momentum, angular velocity and their derivatives for NGC 3198 based on the data shown previously. The blue lines use the fit for v_ϕ rather than the data. The orange line shows the radius of the ring and the purple line shows the bar, as detailed in the text.

fit rather than the observed data from Schmidt et al. (2016). Unfortunately we do not have a lot of data describing the area within the ring, but the line is included, as some information might be gleaned from it.
We can see from this figure that the fit is mostly good. The data appears to deviate significantly from the fit for dJ/dR, but the differences don't make a huge difference in the end, as we'll see. The first point of both the angular velocity data and its derivative don't seem to fit, but that is not surprising considering the error on the first two points in the input data, which was shown in chapter 3.
Next we have the surface density, torque derivative, torque and kinematic viscosity as calculated in chapter 2. The surface density data from Schmidt et al. (2016) was not included in the input data, but using eq. 2.4 it was be recovered for comparison with the data from Leroy et al. (2008) to make sure there are no issues with the data or our calculations. The two sets of data are in decent agreement here, but unfortunately there are issues with some of the other galaxies. These are all the quantities required to calculate α_1. The last quantity needed to calculate α_2 is the scale height H which is shown on fig. 4.3
Finally we have the two different sets of α values. Each α function is calculated three times, first using purely the data from Schmidt et al. (2016), then the rotation curve fit but still using the surface density derived from Schmidt et al. (2016) and

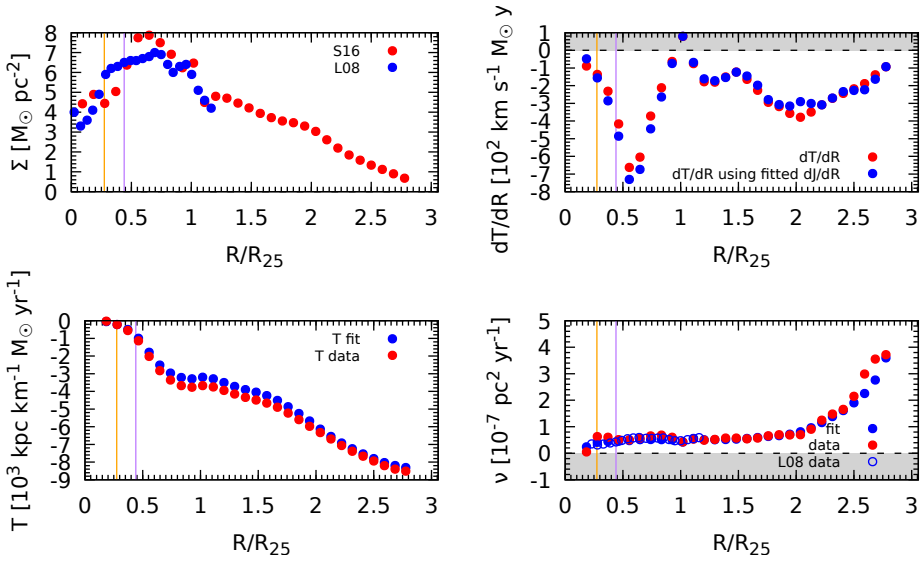

Figure 4.2: Surface density, torque derivative, torque and kinematic viscosity of NGC 3198. The blue dots on the surface density plot use data from Leroy et al. The blue dots on the other one use the rotation curve fit.

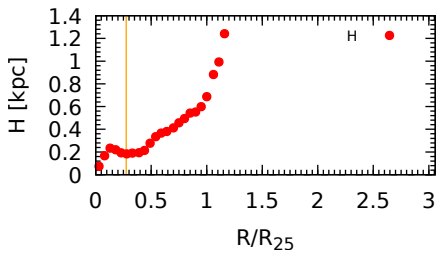

Figure 4.3: The scale height for NGC 3198.

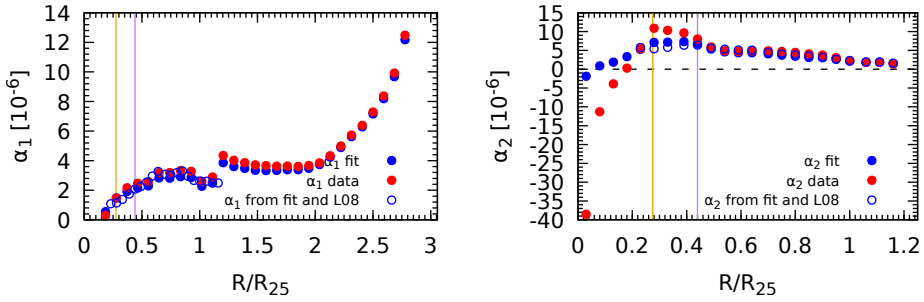

Figure 4.4: α calculated in two different ways.

finally using that fit as well as surface density data from Leroy et al. (2008), which appears to be more accurate than the surface density calculated from the input data. The data from Leroy et al. has a shorter range, so the third set of α_1 and all of the α_2 values don't go any further than $1.2R_{25}$. The sudden jump at that point in α_1 occurs due to the fact that the velocity dispersion data from Romeo & Mogotsi (2017) also only extends to $1.2R_{25}$ and a constant approximation of $11km/s$ was used for the points further from the galactic center.

4.3 The other galaxies (and their data quality)

All of the plots shown for NGC 3198 are shown below for the other nine galaxies. All of the data was analyzed and each galaxy was given a grade from one to five. The first four, NGC 2841, NGC 3521, NGC 5055 and NGC 7331 have data that seems exceptionally good and were given grades ranging from three to five, and are studied in greater detail in the next chapter. The others have various problems which make the data less reliable and as such will not be studied in as much detail. The grade is shown in parentheses in the section titles and the title of each figure. NGC 3198 was given a five star grade.

4.3.1 NGC 2841 ($\star\star\star\star\star$)

NGC 2841 is an unbarred spiral galaxy about $14.1Mpc$ away with a optical radius of $14.2kpc$. It has a prominent ring at a radius of about $4kpc$. It has a ring at a radius of $3.563kpc$ which like earlier is shown on the plots as an orange line. Like many of the other rings in these galaxies, it is too close to the galactic center to be of much use, since only a few data points are within its radius. The galaxy seems to have inflow between 0.5 and $2.75R_{25}$ with most of it at the higher end of this range. The outer areas of the disc seem to flowing outwards quite rapidly and there is also a high radial velocity outwards near the ring radius although there apparently isn't much mass flow. The fit seems very good and the surface densities also seem to agree. This is one of the galaxies looked at in greater detail later.

4.3.2 NGC 3521 ($\star\star\star\star\star$)

This is an intermediate spiral galaxy around $8Mpc$ from Earth with an optical radius of $12.94kpc$. It has both a ring and a bar, although both structures are quite weak, and it has a rather loose spiral structure. The bar is in the purple area on the figures, and is unfortunately rather close to the center. The ring is outside that. NGC 3521 is dominated by inflow, with a small region of outflow around $1.75R_{25}$. The data seems pretty good, the fit is quite close to the actual data and the two sets of surface density data appear to be mostly in agreement. α_1 seems to act strangely at high radii, and including those datapoints makes it hard to see the much smaller details below $1.25R_{25}$ but overall the data seems good enough to be studied further.

4.3.3 NGC 5055 ($\star\star\star$)

NGC 5055 is another unbarred, relatively loosely wound spiral and is about $9Mpc$ from Earth. It has an optical radius of $17.26kpc$. It appears to have a ring or tight spiral at a radius of $1.746kpc$,(Thornley & Mundy, 1997) which is shown on the plots as a vertical orange line like other rings included so far. It should be noted however that much like the ring in 2841, this radius is smaller than the radial coordinate of most of the data points, so its use in our analysis is rather limited. Accretion is common in the inner parts of the disc, within $2.75R_{25}$ but there is significant outflow in the outermost part, similar to many of the other galaxies. Star formation is quite high and then decreases sharply in the outermost regions. While the fit could be better for $\frac{dJ}{dR}$, it is overall very good. There are some discrepancies between the two sets of surface density data but it's not too bad. Overall, this data was considered good enough to be included in further study of the α values.

4.3.4 NGC 7331 ($\star\star\star$)

NGC 7331 is an unbarred spiral about $12Mpc$ away with an optical radius of $19.5kpc$. Interestingly, this galaxy has a counter-rotating bulge (Prada et al., 1996). There is a ring with a radius of $3.5kpc$(Israel & Baas, 1999) which is shown on the figures. There is also a small bar, but as extends less than $1kpc$ from the center it is far too small to be relevant to our analysis. The inner part of the disc is dominated by outflow, increasing linearly to a maximum of about $-3.5M_{\odot}yr^{-1}$ at $0.6R_{25}$. It then switches quickly to inflow, with a maximum of around $3M_{\odot}yr^{-1}$ at $0.8R_{25}$. Note that the mass flow has large error bars, however, so this may not be too precise. The star formation rate is pretty much constant between 0.2 and $1.2R_{25}$. The fits seem pretty good, and the two sets of surface density data seem to mostly agree. The data for this galaxy seems very reliable so it has been included in the further analysis below.

4.3.5 NGC 925 ($\star\star$)

NGC 925 is a loosely wound barred spiral with no ring structure about $9.3Mpc$ away with an optical radius of $14.34kpc$. The bar has a radius of about $3.2kpc$,(Elmegreen & Elmegreen, 1985) and is shown on the plots as a purple line. According to the

data from Schmidt et al. outflow is dominant at most radii, increasing dramatically above $1.2R_{25}$. Looking at the derivatives, some problems become apparent, as the fit for J, Ω and especially their derivatives doesn't seem as good as for many of the other galaxies. Furthermore, looking at the surface density, the calculated values seem almost anticorrelated with the data provided by Leroy et al. at low radii. While the α_1 values don't seem too badly affected for the most part, there are some significant differences in α_2 below $0.6R_{25}$. As a result of these issues, the data for this galaxy is not considered reliable enough.

4.3.6 NGC 2403 ($\star\star$)

NGC 2403 is an intermediate spiral galaxy and is about $2.5Mpc$ away. Its optical radius is $7.38kpc$ and it has a bar with a radius of $1.321kpc$. The data for this one reaches quite far, out to approximately $15R_{25}$, so it reaches much further than the surface density data from Leroy et al. which only goes to $1.2R_{25}$. The accuracy of the data at such high radii is unknown. This galaxy seems to be dominated by inflow at all radii, with maximum accretion around roughly 1, 3, and $6R_{25}$. The fits are better than for NGC 925 but the calculated surface density is almost an order of magnitude lower than the observed surface density from Leroy et al. (2008) which seems very suspicious and calls the reliability into question.

4.3.7 NGC 6946 ($\star\star$)

NGC 6946 is an intermediate spiral with an optical radius of $9.8kpc$, about $7.7Mpc$ (Eldridge & Xiao, 2019) away. It has very little outflow, and interestingly, the inflow is highest at relatively large radii, the opposite of most of the other galaxies studied here. There is a large difference between our fit to the rotation curve and the fit given by Leroy et al. and the fit doesn't seem particularly accurate due to its limitations and the shape of the rotation curve. there is also an interesting lack of star formation below $0.5R_{25}$. The problem with the inaccurate fit propagates as can be seen in the plots for J, Ω and their derivatives, $\frac{dJ}{dR}$ in particular.
The surface densities again show anticorrelation and an order of magnitude difference around $0.5R_{25}$. The scale height seems far lower than it should be, and there are substantial differences in the shape of the α values simply due to the differences in the data. Overall, this data seems very unreliable where it exists.

4.3.8 NGC 2903 ($\star$)

NGC 2903 is a barred spiral galaxy $9.4Mpc$ away and it has an optical radius of $15.21kpc$. Its data is unfortunately not usable because the surface density from Leroy et al. is missing, as is the velocity dispersion from Romeo & Mogotsi (2017). The lack of the total surface density data means that the scale height and α_2 cannot be calculated. The quantities that could be calculated are included and seem to be quite interesting, with significant amounts of both inflow and outflow and a very sharp rise in star formation rate around $0.5R_{25}$.

4.3.9 NGC 3621 ($\star$)

NGC 3621 is an unbarred, loosely wound spiral 6.64 Mpc away from Earth with an optical radius of $9.38kpc$. It has both inflow and outflow alternating through the disc, with a maximal inflow of almost $2M_{\odot}yr^{-1}$ near $1.3R_{25}$ and a maximal outflow of around $-3M_{\odot}yr^{-1}$ near $4R_{25}$. The star formation rate is relatively consistent across the entire range, with slightly more in the inner parts of the disc. This galaxy unfortunately has the same issue as NGC 2903. There is no surface density for it given by Leroy et al. meaning that α_2 cannot be calculated. The velocity dispersion data is also missing for this one and while an approximation can be used, it obviously reduces the accuracy of the data.

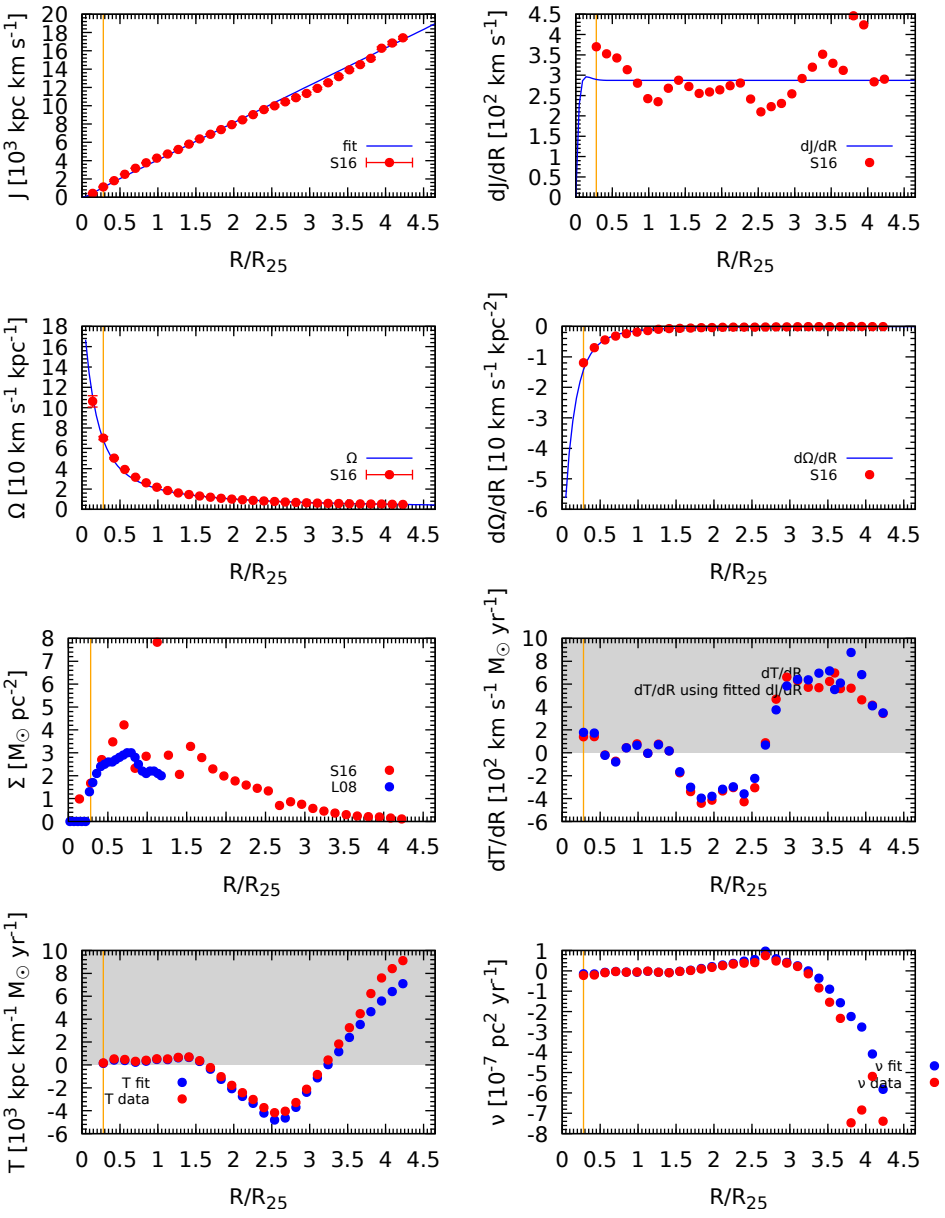

Figure 4.5: The first eight output quantities for NGC 2841. The vertical orange line shows the radius of the ring.

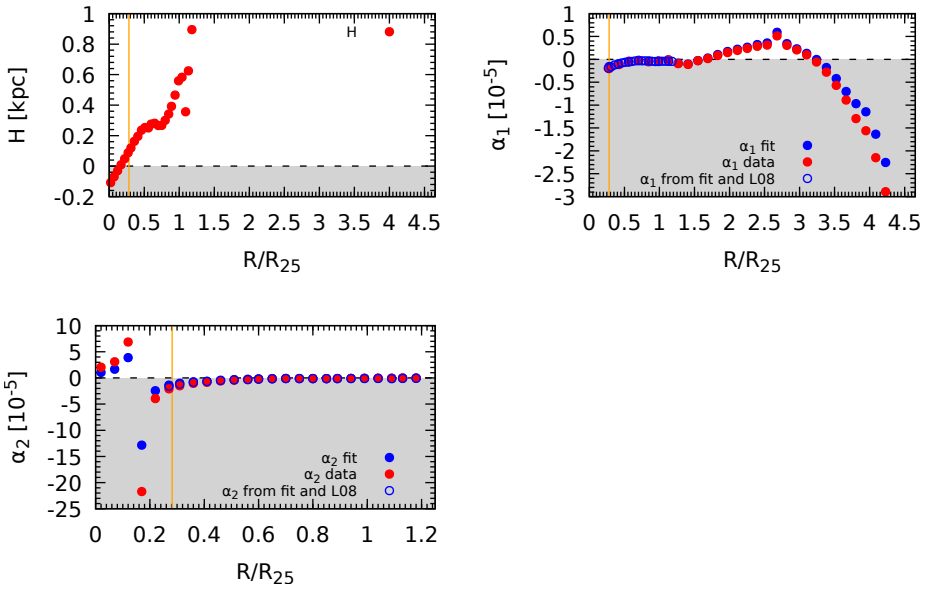

Figure 4.6: The scale height and α values for NGC 2841.

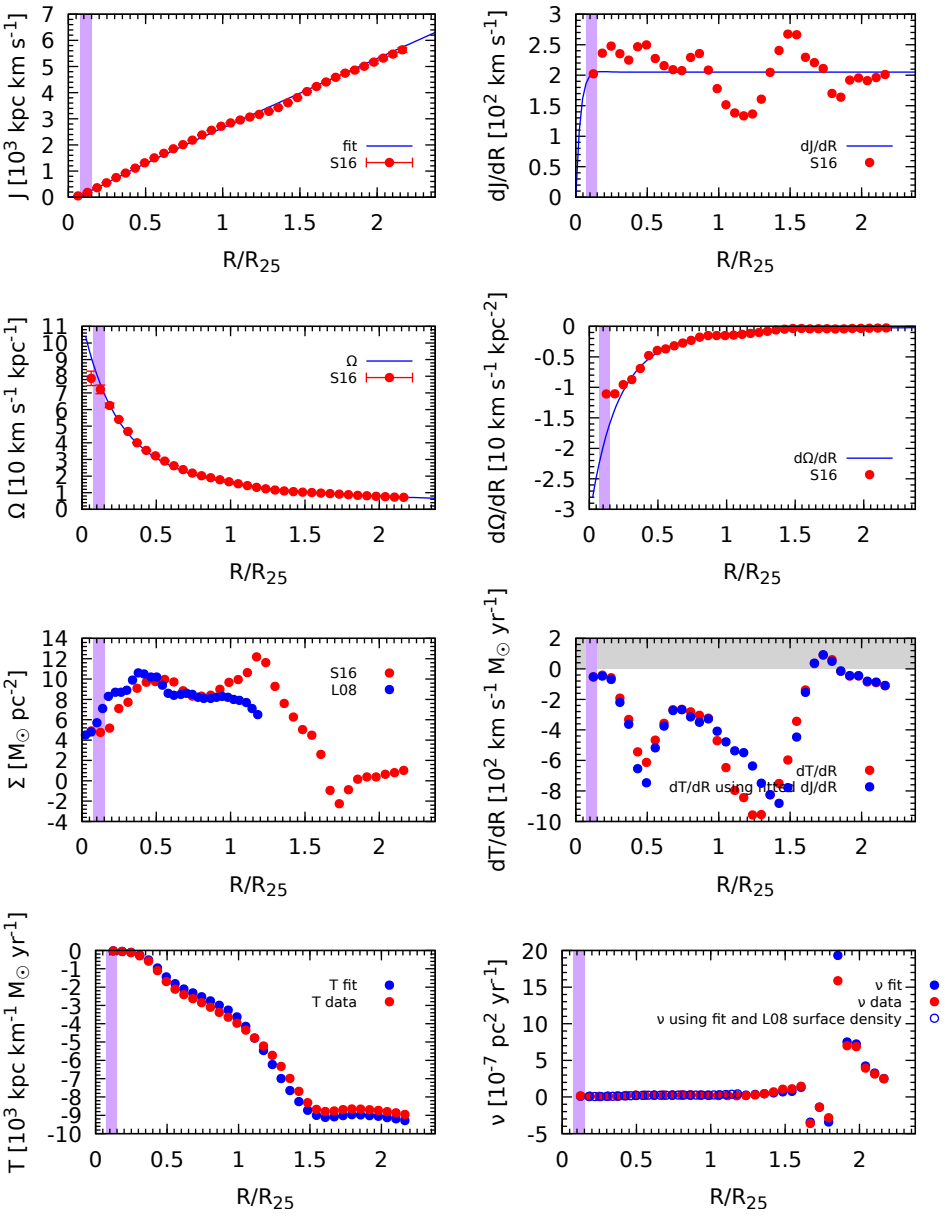

Figure 4.7: The first eight output quantities for NGC 3521. There is a bar around $0.970 - 1.939 kpc$, shown as a purple area.

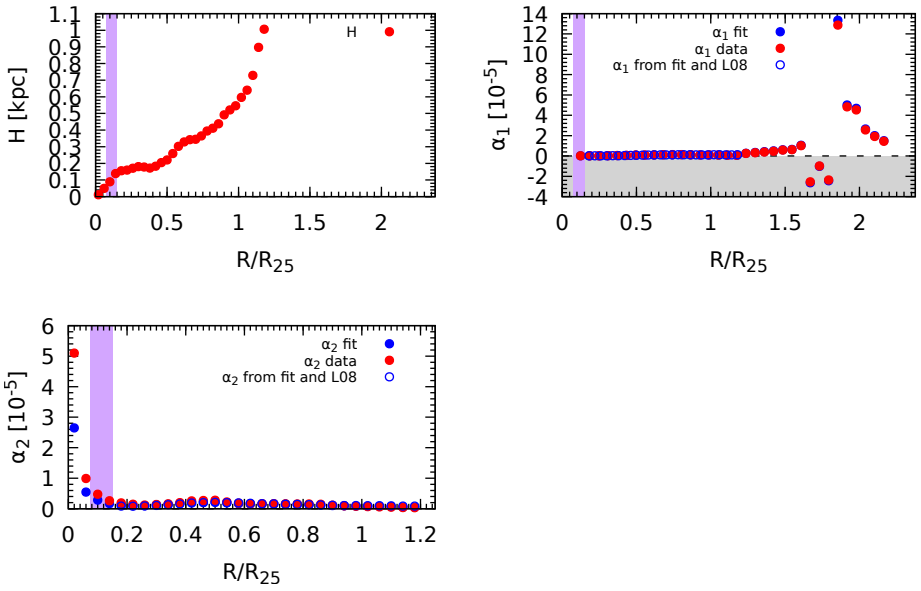

Figure 4.8: The scale height and α values for NGC 3521.

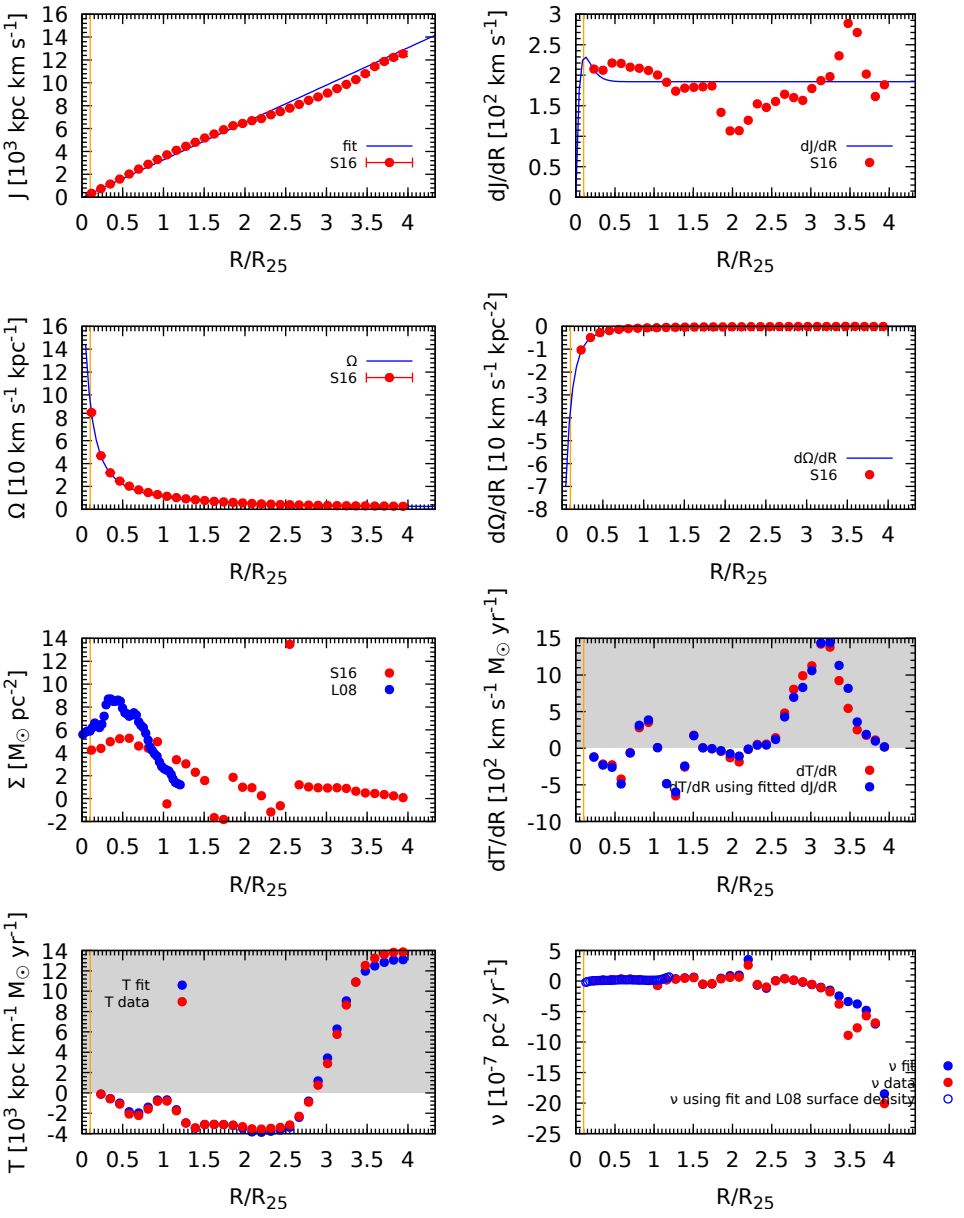

Figure 4.9: The first eight output quantities for NGC 5055.This galaxy also has a ring at a radius of around 1.746kpc, shown as an orange line.

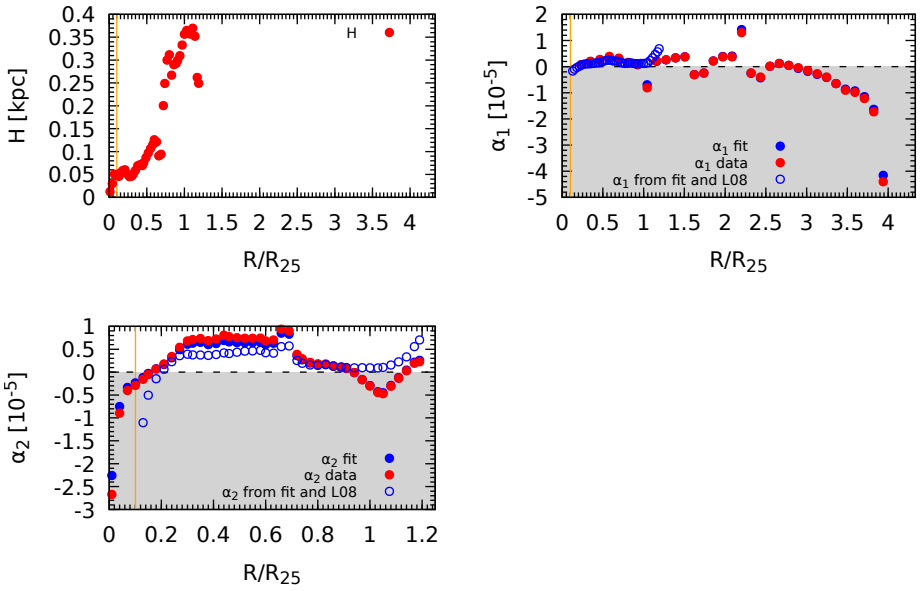

Figure 4.10: The scale height and α values for NGC 5055. The ring is shown as an orange line.

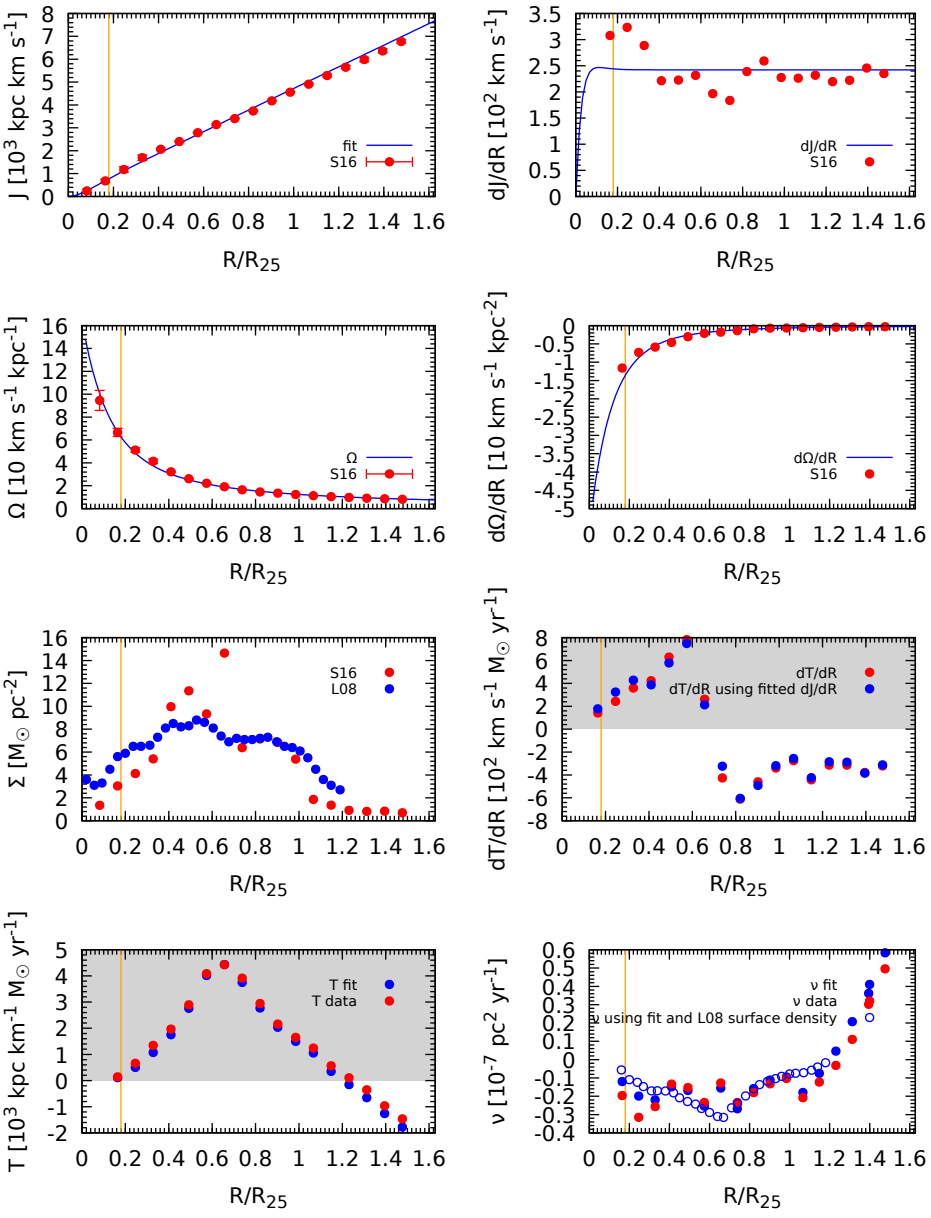

Figure 4.11: The first eight output quantities for NGC 7331.

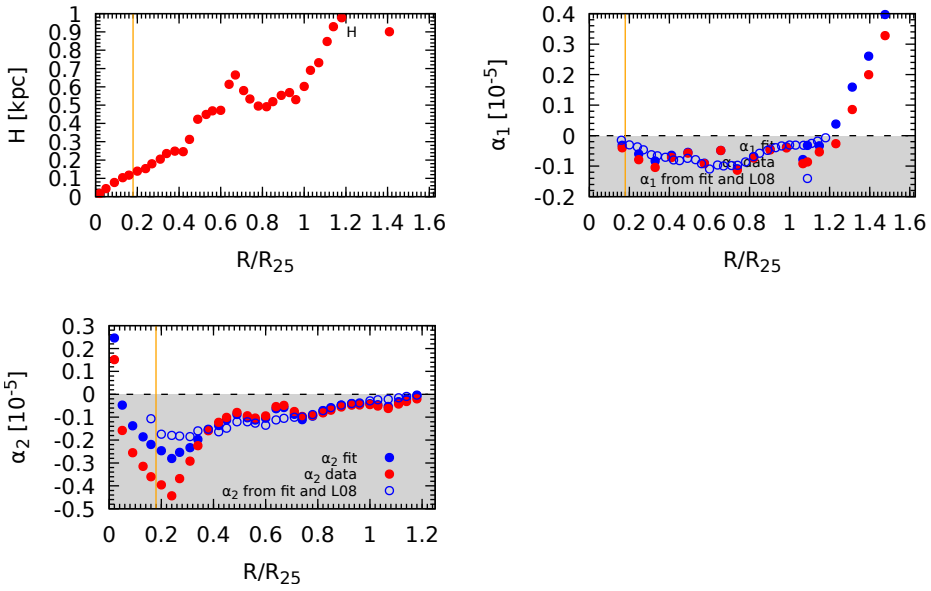

Figure 4.12: The scale height and α values for NGC 7331.

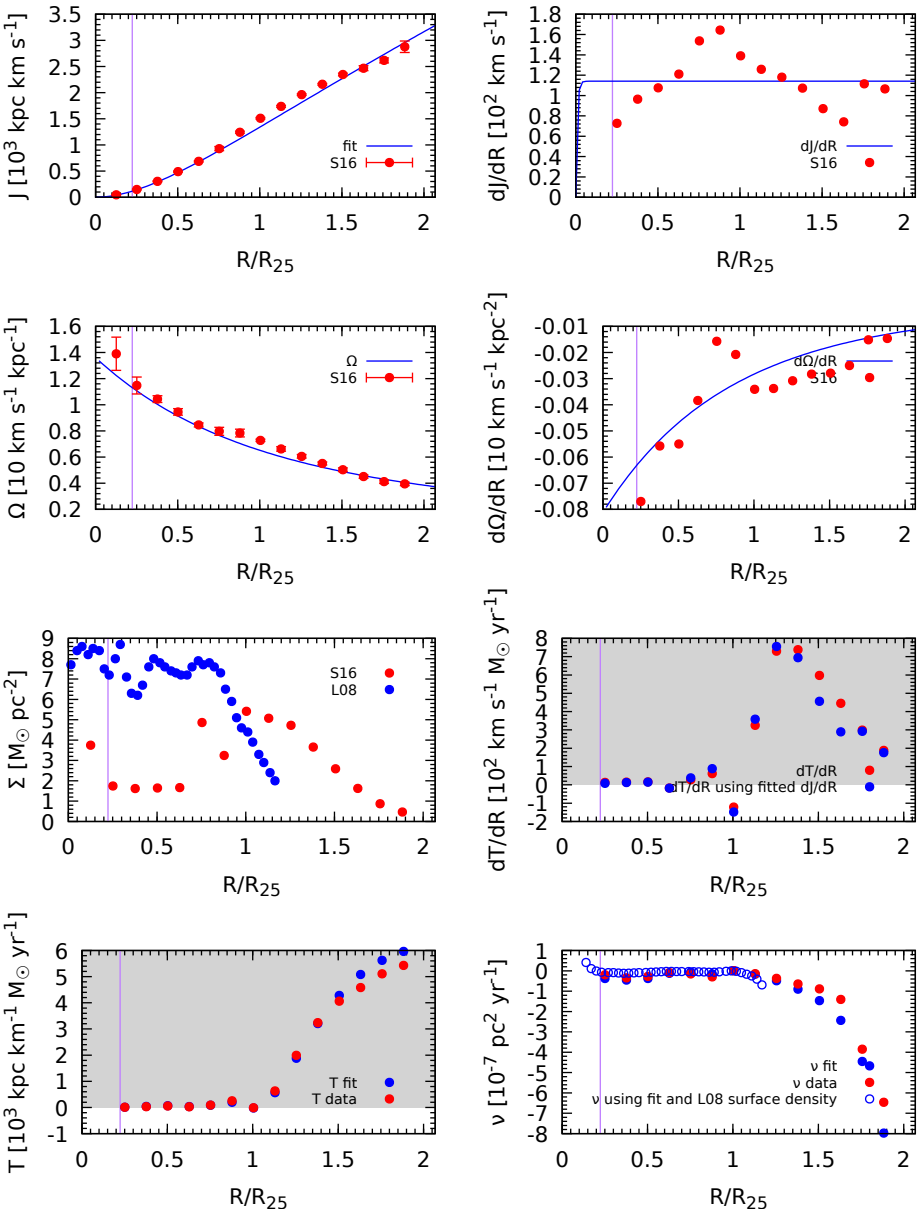

Figure 4.13: The first eight output quantities for NGC 925. The purple line shows the radius of the bar.

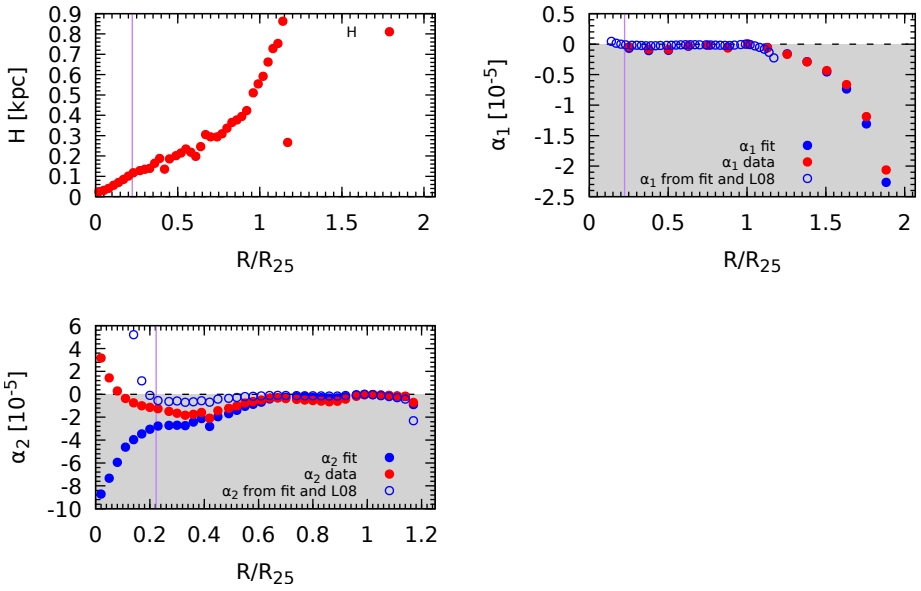

Figure 4.14: The scale height and α values for NGC 925.

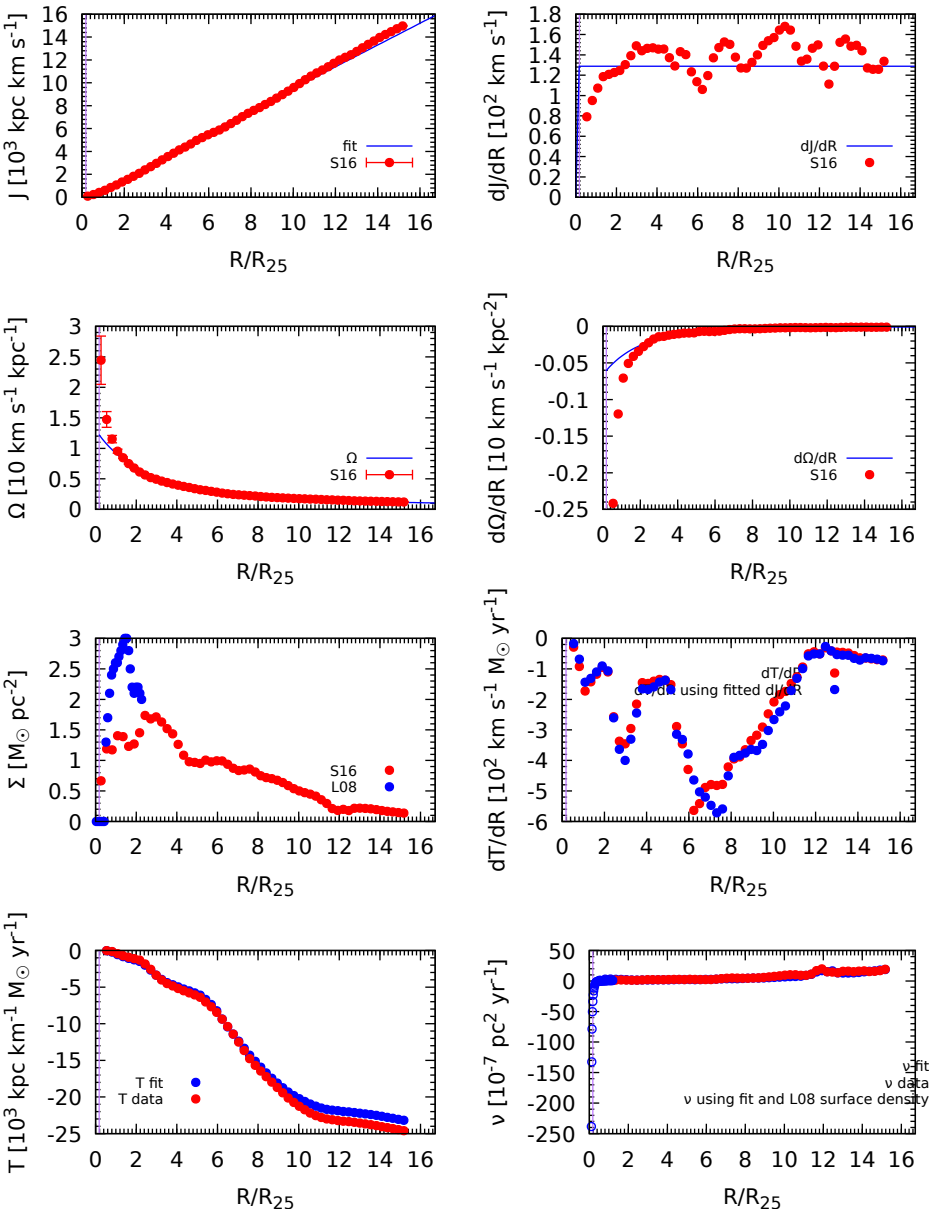

Figure 4.15: The first eight output quantities for NGC 2403. There is a bar shown in purple

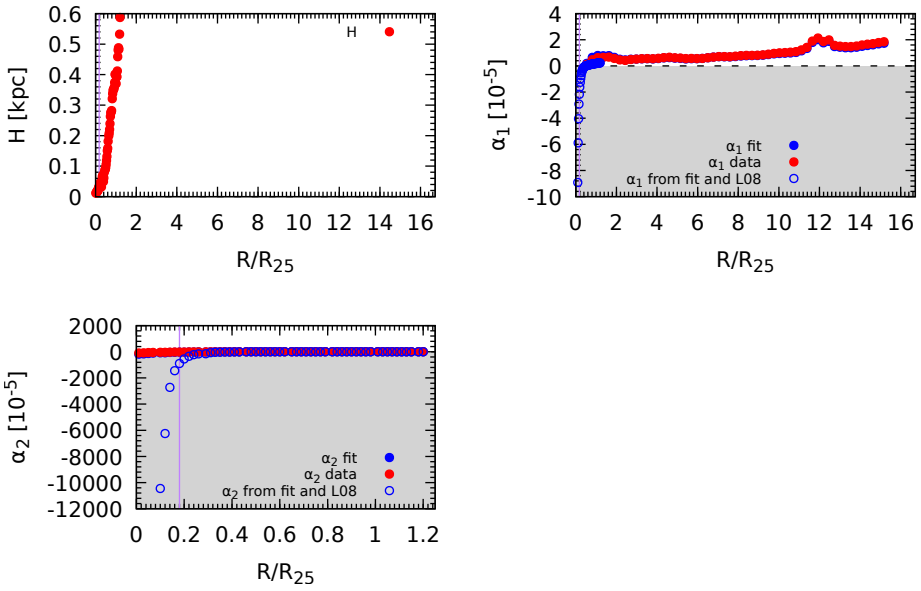

Figure 4.16: The scale height and α values for NGC 2403.

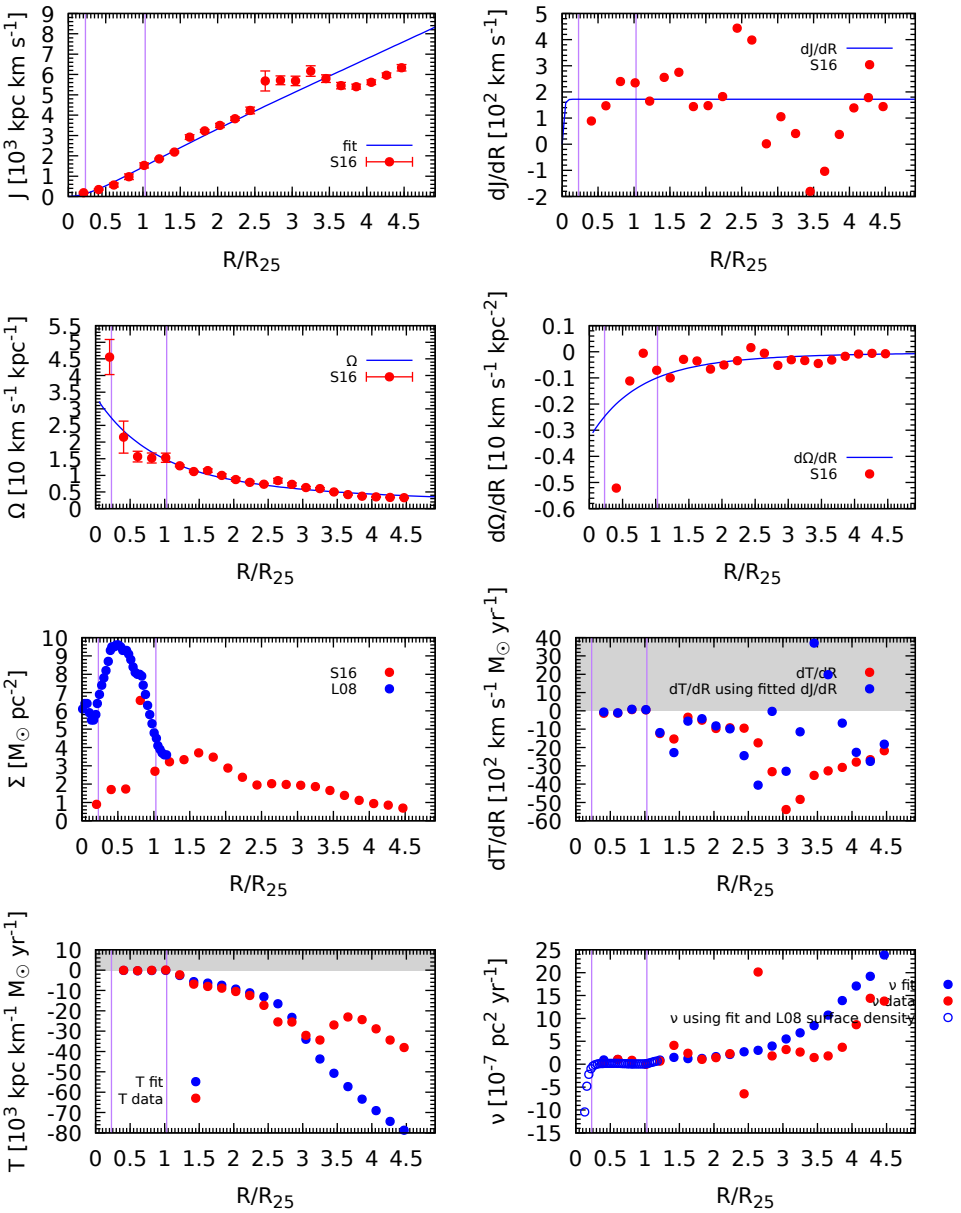

Figure 4.17: The first eight output quantities for NGC 6946.

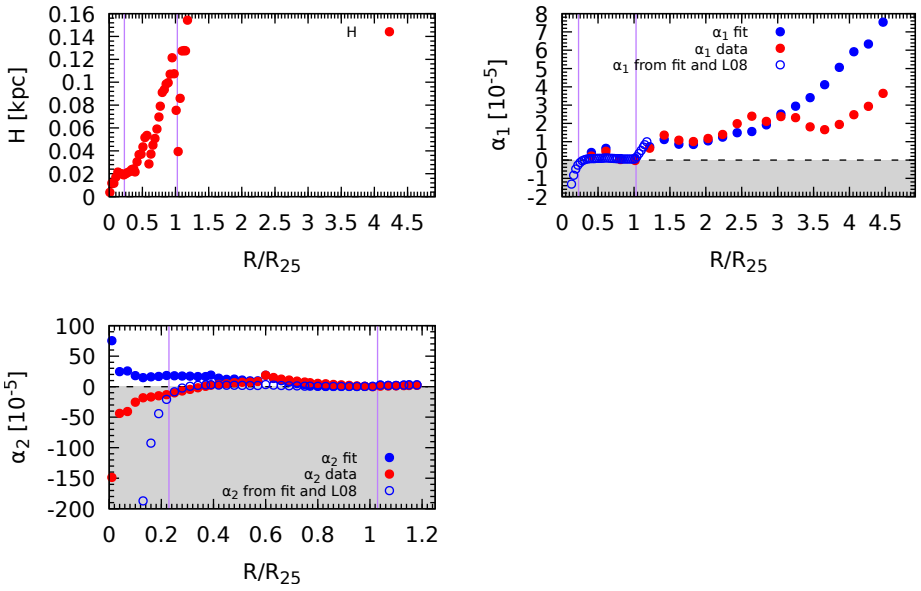

Figure 4.18: The scale height and α values for NGC 6946.

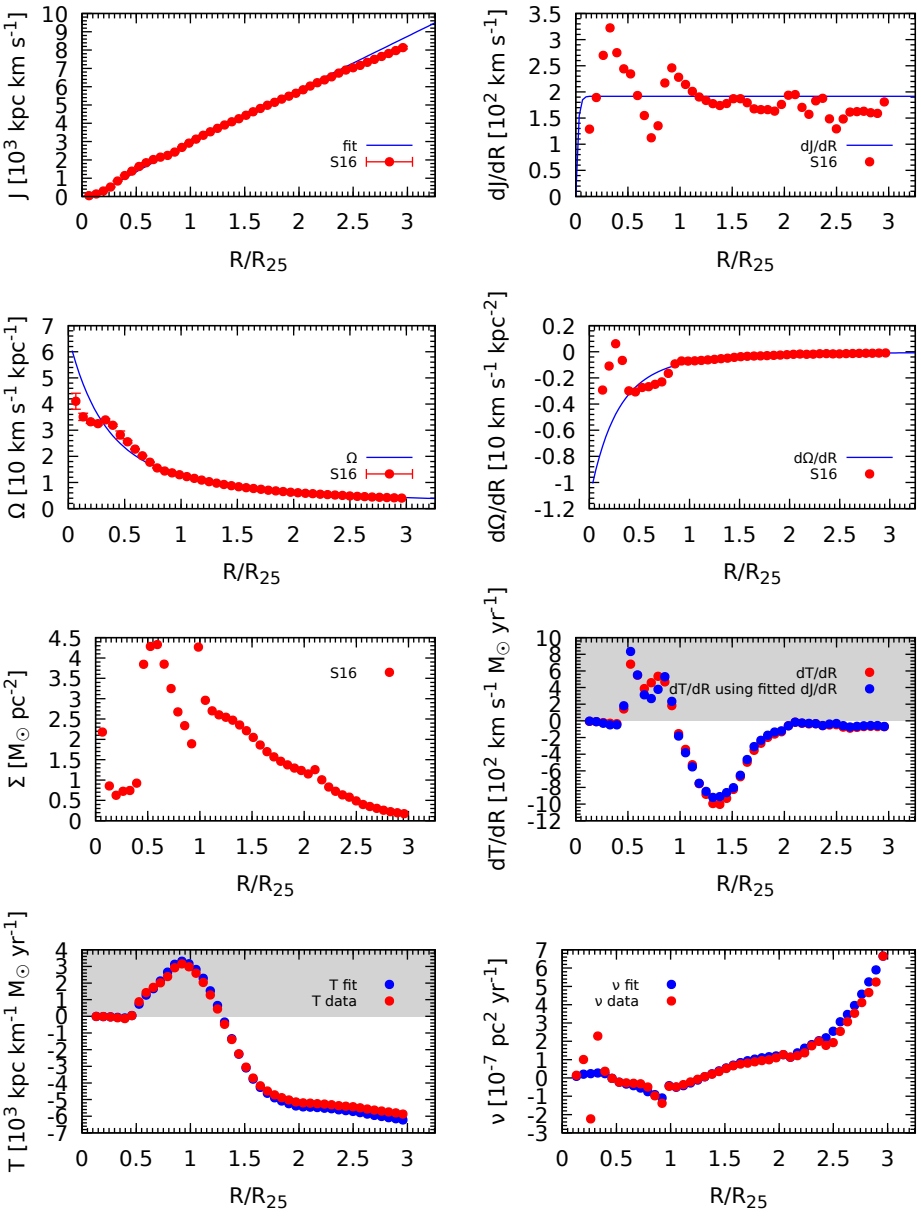

Figure 4.19: The first eight output quantities for NGC 2903.

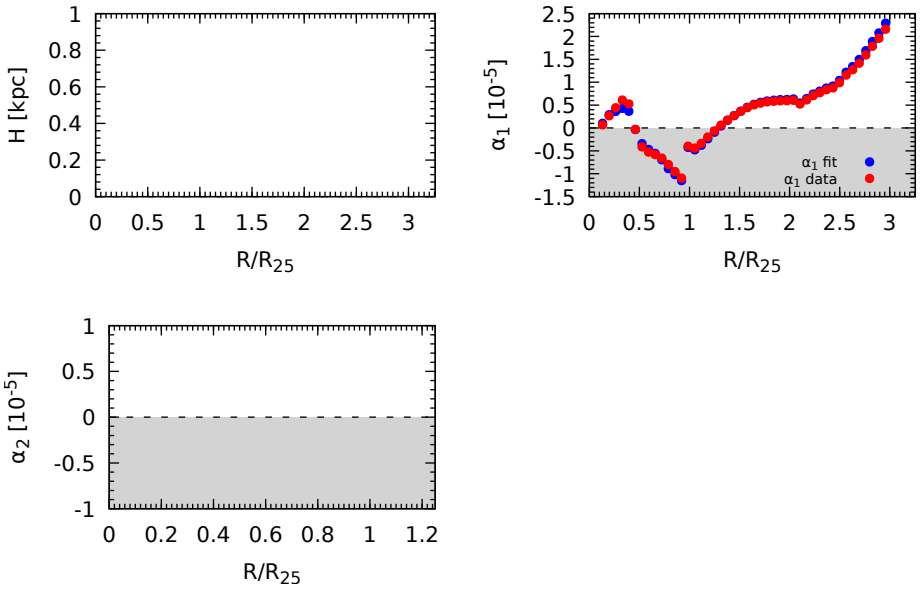

Figure 4.20: The scale height and α values for NGC 2903.

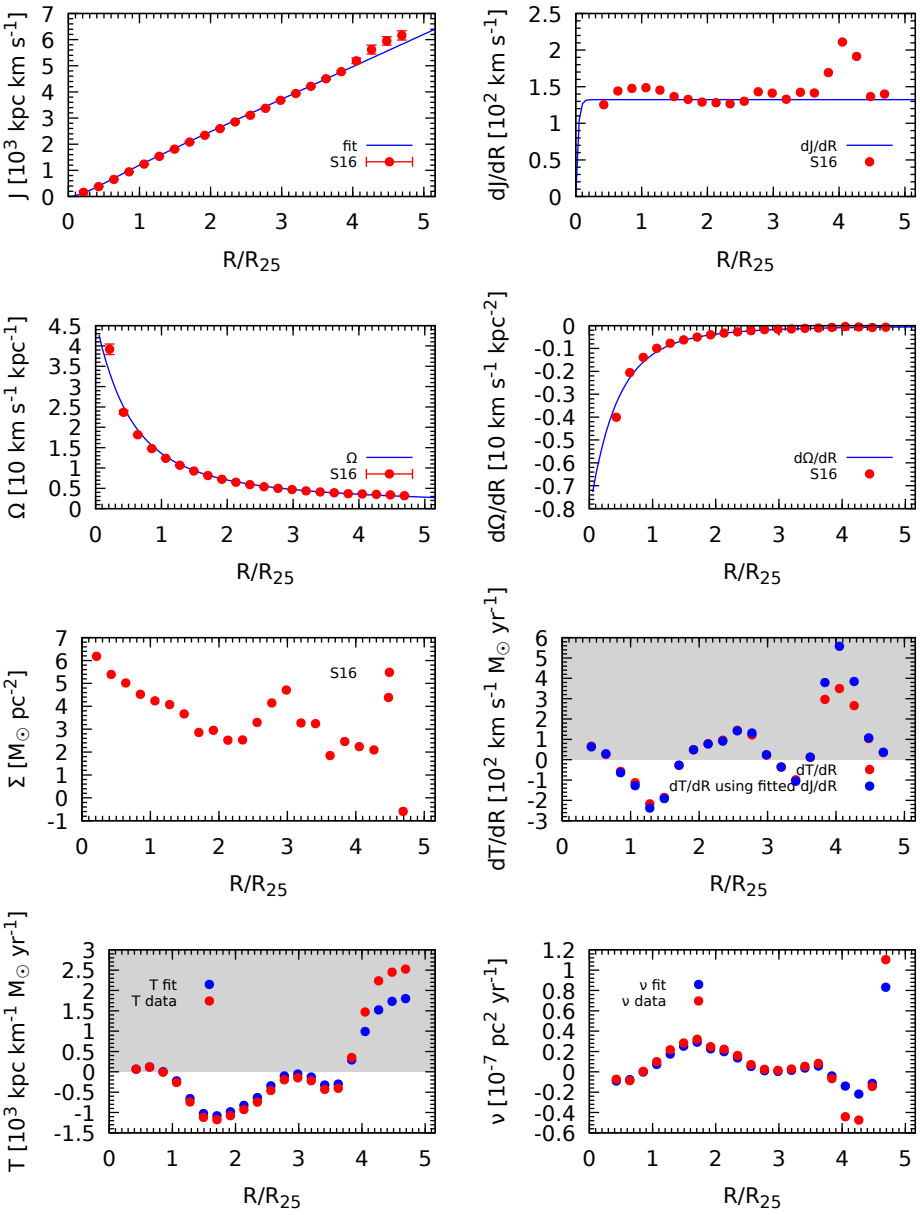

Figure 4.21: The first eight output quantities for NGC 3621.

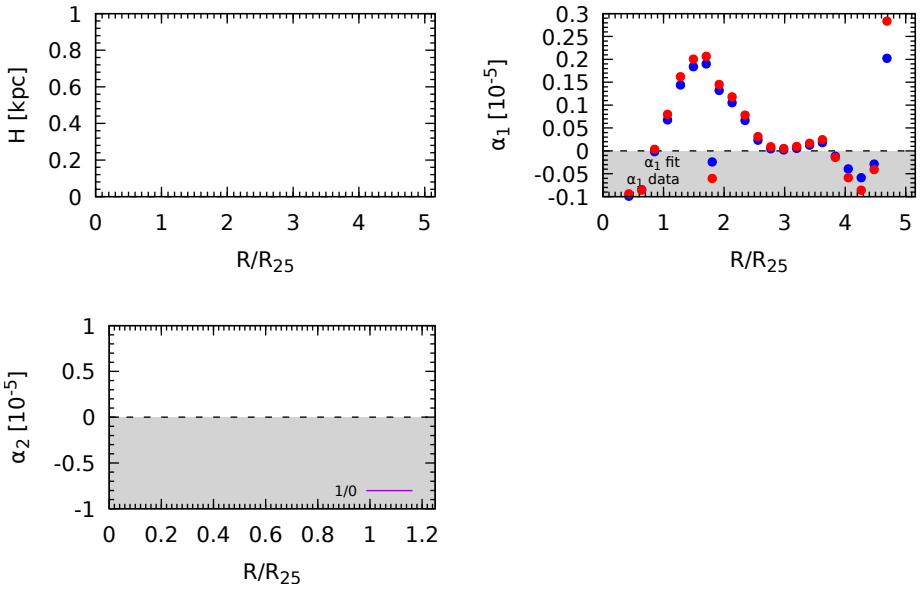

Figure 4.22: The scale height and α values for NGC 3621.

5

Astrophysical Implications

Now that the α values for these galaxies have been calculated and plotted along with the other relevant quantities, can we see the effects that a galaxy's structure has on α? Tables 5.1 and 5.2 show single representative α values for each of the 5 galaxies where the quality of the results was considered good enough to warrant further analysis. Each α_1 and α_2 was calculated eight times, using four different methods, with the first set on table 5.1 using solely the points with a positive sign representing inflow and the second set on table 5.2 using the points with a negative sign which represent outflow. The methods used are simply a median, a mean, a mass weighted average, and the maximum/minimum values, i.e. the points with the largest absolute distance from 0. In galaxies where there is no mass flow in a particular direction, the space is left empty. Unsurprisingly, inflow is dominant in most galaxies, so the outflow table is significantly less complete. On each table, galaxies dominated by flow in the opposite direction are colored grey. The way the table entries are calculated, the grey entries may be made up of outliers which aren't representative of the galaxy as a whole.

5.1 Is there a correlation between galaxy structures and α?

5.1.1 Implications of radial profiles of α

Looking at the first galaxy, NGC 3198, it has both a ring and a bar. The ring is rather close to the center, but we can some potentially interesting things, particularly regarding α_2. It appears to increase rapidly from the first data points to the ring, where it either reaches a maximum, levels out or slows down the increase depending on which points are used. At the end of the bar, the 3 lines have practically converged and all decrease relatively steadily with increasing distance. We see from this that the greatest efficiency is seemingly outside the ring but inside the bar. α_1 is seemingly not effected by those structures. It reaches a maximum between approximately 0.6 and $0.9R_{25}$. As previously mentioned, the jump at $1.2R_{25}$ is due to the velocity dispersion data from Romeo & Mogotsi (2017) ending and an approximate value of $11km/s$ being used instead. It appears that the accretion efficiency increases by a huge amount at very high radii but the results aren't necessarily all that reliable at very large radii. α_2 seems far more interesting due to the smaller radius of more reliable data, and the strong effects of the structures.
NGC 2841 is rather interesting, since as can be seen on the input figures, it is

dominated by outflow, which reverses the sign. This galaxy is unbarred, so we only have the ring to look at. α_1 is not very interesting in that regard, since there is only one point in within the ring, which can be said to agree somewhat with the α_2 data, but doesn't show much. The area of inflow can be seen clearly, followed by a drop which seems similar to the rise at high radii in NGC 3198, albeit in the opposite direction. α_2 shows a sharp rise within the ring, and then slow, asymptotic behavior beyond it to the maximum of $1.2R_{25}$. This plot does not extend far enough to show the inflow area. Bearing in mind that the α values here are negative, it appears to be inverted compared to NGC 3198. The magnitude of α_2 decreases sharply until it quickly evens out, the shift happening when around the radius of the ring. In NGC 3198, α_2 increased out to the ring.
The α_1 plot of NGC 3521 does not seem particularly useful, since the massive jumps at high radii flatten the rest. α_2 does show some results. While there is no data within the radius of the bar, we do see that around the area where the bar ends there is a distinct drop, possibly comparable to the drop after the bar in NGC 3198. There is not an obvious explanation for the rise to a maximum around $0.5R_{25}$, however, and there may be some structures not accounted for on the plot.
NGC 5055 unfortunately only has a ring very close to the center, which isn't very useful. We can see that α increases and goes from negative to positive just after the ring. NGC 7331 also only has a ring, and there the results are also inconclusive. We don't see any definite changes in α at that radius.

5.1.2 Implications of characteristic values of α

Let's look at the inflow first. There are some issues with some of the data. For instance, looking at α_1, NGC 3521 tends to have the smallest median and mass weighted average, but largest mean and maximum. This is obviously due to the strange scattering of data points at high radii, so we probably shouldn't look too seriously at that. The outflow and α_2 still seems decently reliable though. NGC 3521 and 5055 have similar spiral arms, though only the former has a sort of bar. We do not, however, see this reflected in the tables, where there is no more of a connection between them than any of the others. NGC 2841 has the most tightly wound spiral arms of the four while NGC 3198 has the least wound.
Therefor, it appears we cannot link the α values to the type of spiral arms, at least not with the sample size we have here.
We can see that the outflow α values in the outflow dominated galaxies tend to be smaller than the inflow α of those galaxies where inflow is dominant. From this we see that the outflow dominated discs appear to be less viscous and the angular momentum transfer is less efficient.
The range in α values for stellar scale accretion discs is thought to be about $0.01-0.4$ (King et al., 2007). The tables above show values which are consistently of the order of $10^{-7}-10^{-5}$. We can see that the α values of galactic discs are about $4-5$ orders of magnitude lower than those of the stellar scale discs. This result is not unexpected as the scale and low density of galactic discs means that the only forces driving the transfer of angular momentum are gravitational forces working over vast distances.

Inflow

Median

	$\alpha_{1,S16}$	$\alpha_{1,L08fit}$	$\alpha_{1,L08data}$	$\alpha_{2,S16}$	$\alpha_{2,L08fit}$	$\alpha_{2,L08data}$
NGC 3198	3.38e-06	3.66e-06	2.61e-06	3.58e-06	4.72e-06	4.47e-06
NGC 2841	2.32e-06	2.06e-06	—	1.67e-05	3.1e-05	—
NGC 3521	1.11e-06	1.25e-06	1.06e-06	1.46e-06	1.61e-06	1.3e-06
NGC 5055	2.34e-06	2.39e-06	1.41e-06	5.45e-06	6.12e-06	3.46e-06
NGC 7331	2.1e-06	2e-06	—	2.46e-06	1.52e-06	—

Mean

	$\alpha_{1,S16}$	$\alpha_{1,L08fit}$	$\alpha_{1,L08data}$	$\alpha_{2,S16}$	$\alpha_{2,L08fit}$	$\alpha_{2,L08data}$
NGC 3198	4.06e-06	4.31e-06	2.46e-06	3.91e-06	4.87e-06	4.23e-06
NGC 2841	2.52e-06	2.19e-06	—	2.2e-05	4.01e-05	—
NGC 3521	1.11e-05	1.07e-05	8.29e-07	2.37e-06	3.57e-06	1.35e-06
NGC 5055	2.86e-06	2.86e-06	1.89e-06	4.33e-06	4.83e-06	3.02e-06
NGC 7331	2.14e-06	2.04e-06	—	2.46e-06	1.52e-06	—

Mass-weighted average

	$\alpha_{1,S16}$	$\alpha_{1,L08fit}$	$\alpha_{1,L08data}$	$\alpha_{2,S16}$	$\alpha_{2,L08fit}$	$\alpha_{2,L08data}$
NGC 3198	3.93e-06	4.2e-06	2.68e-06	3.62e-06	4.31e-06	3.76e-06
NGC 2841	2.5e-06	2.17e-06	—	—	—	—
NGC 3521	2.02e-06	1.96e-06	9.67e-07	1.26e-06	1.4e-06	1.33e-06
NGC 5055	2.29e-06	2.27e-06	1.78e-06	4.75e-06	5.33e-06	3.12e-06
NGC 7331	2.29e-06	2.31e-06	—	—	—	—

Maximum

	$\alpha_{1,S16}$	$\alpha_{1,L08fit}$	$\alpha_{1,L08data}$	$\alpha_{2,S16}$	$\alpha_{2,L08fit}$	$\alpha_{2,L08data}$
NGC 3198	1.22e-05	1.25e-05	3.3e-06	7.33e-06	1.09e-05	6.43e-06
NGC 2841	5.91e-06	5.15e-06	—	3.87e-05	6.87e-05	—
NGC 3521	0.000134	0.000129	1.23e-06	2.65e-05	5.1e-05	2.1e-06
NGC 5055	1.42e-05	1.3e-05	6.82e-06	8.52e-06	9.39e-06	7.03e-06
NGC 7331	3.97e-06	3.28e-06	—	2.46e-06	1.52e-06	—

Table 5.1: Individual α values for each galaxy based solely on inflow. Galaxies highlighted in grey are dominated by outflows, so the inflow values are based largely on outliers and not necessarily representative of the galaxy overall.

Outflow

Median

	$\alpha_{1,S16}$	$\alpha_{1,L08fit}$	$\alpha_{1,L08data}$	$\alpha_{2,S16}$	$\alpha_{2,L08fit}$	$\alpha_{2,L08data}$
NGC 3198	—	—	—	-1.86e-06	-1.13e-05	—
NGC 2841	-9.75e-07	-1.13e-06	-4.3e-07	-1.34e-06	-1.51e-06	-1.31e-06
NGC 3521	-2.45e-05	-2.36e-05	—	—	—	—
NGC 5055	-4.3e-06	-3.98e-06	-9.88e-07	-2.9e-06	-3.06e-06	-5.04e-06
NGC 7331	-6e-07	-6.47e-07	-6.26e-07	-9.17e-07	-9.31e-07	-1.05e-06

Mean

	$\alpha_{1,S16}$	$\alpha_{1,L08fit}$	$\alpha_{1,L08data}$	$\alpha_{2,S16}$	$\alpha_{2,L08fit}$	$\alpha_{2,L08data}$
NGC 3198	—	—	—	-1.86e-06	-1.79e-05	—
NGC 2841	-4.4e-06	-5.79e-06	-6.15e-07	-9.67e-06	-1.54e-05	-3.38e-06
NGC 3521	-2.04e-05	-1.96e-05	—	—	—	—
NGC 5055	-8.18e-06	-8.49e-06	-1e-06	-4.21e-06	-4.86e-06	-5.84e-06
NGC 7331	-6.18e-07	-6.71e-07	-5.91e-07	-1.09e-06	-1.4e-06	-9.71e-07

Mass-weighted average

	$\alpha_{1,S16}$	$\alpha_{1,L08fit}$	$\alpha_{1,L08data}$	$\alpha_{2,S16}$	$\alpha_{2,L08fit}$	$\alpha_{2,L08data}$
NGC 3198	—	—	—	—	-8.99e-06	—
NGC 2841	-1.63e-06	-2.13e-06	-4.9e-07	-1.76e-06	-2.18e-06	-2.15e-06
NGC 3521	-1.59e-05	-1.53e-05	—	—	—	—
NGC 5055	-9.27e-06	-9.52e-06	-8.02e-07	-2.42e-06	-2.6e-06	-4.36e-06
NGC 7331	-6.25e-07	-6.65e-07	-6.22e-07	-8.53e-07	-9.37e-07	-8.37e-07

Minimum value

	$\alpha_{1,S16}$	$\alpha_{1,L08fit}$	$\alpha_{1,L08data}$	$\alpha_{2,S16}$	$\alpha_{2,L08fit}$	$\alpha_{2,L08data}$
NGC 3198	—	—	—	-1.86e-06	-3.85e-05	—
NGC 2841	-2.25e-05	-2.89e-05	-1.93e-06	-0.000128	-0.000217	-1.56e-05
NGC 3521	-2.64e-05	-2.54e-05	—	—	—	—
NGC 5055	-4.16e-05	-4.4e-05	-1.68e-06	-2.26e-05	-2.67e-05	-1.1e-05
NGC 7331	-1.09e-06	-1.13e-06	-1.1e-06	-2.8e-06	-4.43e-06	-1.85e-06

Table 5.2: α values based solely on outflow. Galaxies highlighted in grey are dominated by inflows, so the values shown here may not be reliable.

6
Conclusions

We have taken the data given by Schmidt et al. and calculated α values for all of the galaxies for comparison with smaller scale accretion discs and to see what impact galactic structures have on the viscosity of a disc. Perhaps unsurprisingly, the α values of galaxies are many orders of magnitude smaller than those of stellar scale accretion discs, with the former being around $10^{-7} - 10^{-5}$ while the latter tend to be of the order of $10^{-1} - 10^{-2}$. Stars interact purely through gravity, whereas the interactions in stellar scale discs happen through a variety of forces, with magneto-hydrodynamics thought to be particularly important in those cases.

An analysis of the radial α plots found that α tends to start by increasing or falling dramatically, before levelling out at the radius of the ring or the maximum radius of the bar. NGC 3198, possibly the most interesting case out of the ten galaxies, has both a bar and a ring, and there we can see α level out at the radius of the ring, and then seem to stay somewhat steady before falling outside the bar.

Unfortunately, the results do not seem conclusive regarding the effect of spiral structure on α. It does seem likely that spiral structures are influential, but all of the galaxies in the sample are spirals leaving us with limited opportunities to compare radial profiles. There has not been any correlation between α and the type of spiral structure.

Given more time, it would be interesting to examine a larger sample of galaxies. The galaxies used here were all spirals, many with similar spiral types. Some of the galaxies examined were unique within the sample, which makes it very difficult to determine whether or not the behavior of α is common to the type or if it is a result of something else. More galaxies of each type would allow for a more accurate comparison. It might also be informative to compare to a suitable lenticular galaxy.

Another possibility for future study could be to focus on the rings and bars in greater detail. While it can clearly be seen that they influence α, there are some issues barring more extensive study in this thesis. Some of the galaxies do not have the relevant structures and for many of the others, the structures are too close to the center for the data we have to give a complete image. As mentioned in chapter 3, the method used to get the data are somewhat less accurate at very small radii, so it might be worthwhile to investigate different methods with more of a focus on the central regions of the galaxies.

A larger sample size would also make it more practical to look at the inflow and outflow dominated galaxies separately. Tables 5.1 and 5.2 do not make a distinction between galaxies that are dominated by flow in the relevant direction, and galaxies where most of the mass flow is in the opposite direction but there are spikes which may not be accurate representations. It would be ideal to separate these two cat-

egories and only compare outflow dominated galaxies to other outflow dominated galaxies, for instance. Here it is not entirely practical due to the small number of galaxies.
While many things can be gleaned from these results, they are only a beginning and there is a lot more work to be done to get a concrete idea of the impact galactic structures have on the disc viscosity via the α parameter.

Bibliography

Corradi, R. L. M., Boulesteix, J., Bosma, A., Amram, P., & Capaccioli, M. (1991). *A&A*, 244, 27.

Daod, N. A. & Zeki, M. K. (2019). *ApJ*, 870.

Eldridge, J. & Xiao, L. (2019). *MNRAS Letters*, 485, L58.

Elmegreen, B. G. & Elmegreen, D. M. (1985). *ApJ*, 288, 438.

Israel, F. P. & Baas, F. (1999). *A&A*, 351, 10.

King, A. R., Pringle, J. E., & Livio, M. (2007). *MNRAS*, 376, 1740.

Leroy, A. K., F., W., Brinks, E., F., B., de Blok, W. J. G., Madore, B., & Thornley, M. D. (2008). *AJ*, 136, 2782.

Prada, F., Gutierrez, C., Peletier, R., & McKeith, C. D. (1996). *ApJ Letters*, 463, L9.

Pringle, J. E. (1981). *ARA&A*, 19, 137.

Romeo, A. B. (1992). *MNRAS*, 256, 307.

Romeo, A. B. & Mogotsi, K. M. (2017). *MNRAS*, 469, 286.

Ryden, B. (2011). *Radiative Gas Dynamics*. Ohio State University.

Schmidt, T. M., Bigiel, F., Klessen, R. S., & de Blok, W. J. G. (2016). *MNRAS*, 457, 2642.

Shakura, N. I. & Sunyaev, R. A. (1973).

Shu, F. H. (1991). *The Physics of Astrophysics: Gas dynamics*. University Science Books.

Thornley, M. D. & Mundy, L. G. (1997). *ApJ*, 484, 202.

Turner, N. J., Fromang, S., Gammie, C., Klahr, H., Lesur, G., Wardle, M., & Bai, X.-N. (2014). *Protostars and Planets VI*, (pp. 411).